ANALYSIS OF ELECTRON FLOW IN POTENTIAL CHANNEL STRUCTURES DISCONTINUOUS IN TRANSVERSE DIMENSION

BY

KHWAJA MUSTAFIZUR RAHMAN

A THESIS

SUBMITTED TO THE DEPARTMENT OF ELECTRICAL AND ELECTRONIC ENGINEERING IN PARTIAL FULFILMENT OF THE REQUIREMENTS FOR THE DEGREE OF

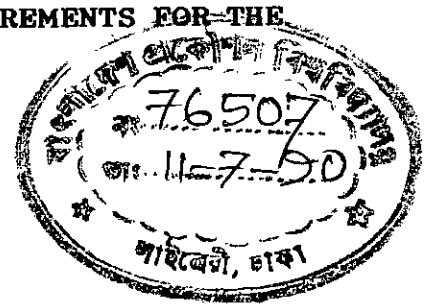

MASTER OF SCIENCE IN ENGINEERING

DEPARTMENT OF ELECTRICAL AND ELECTRONIC ENGINEERING

BANGLADESH UNIVERSITY OF ENGINEERING AND TECHNOLOGY, DHAKA

APRIL, 1990

Accepted as satisfactory in partial fulfilment of the requirement for the degree of Master of Science in Engineering (Electrical and Electronic) of Khwaja Mustafizur Rahman, Roll number 871316P.

BOARD OF EXAMINER

1. _____ Chairman
(Dr. M. Rezwan Khan) (Supervisor)
Associtae professor,
Department of Electrical and
Electronic Engineering,
BUET, Dhaka.

2. _____ 17.4.90. Member
(Dr. Md. Abdul Matin) (Ex-Officio)
Professor and Head,
Department of Electrical and
Electronic Engineering,
BUET, Dhaka.

3. _____ Member
(Dr. M. M. Shahidul Hassan)
Associate Professor,
Department of Electrical and
Electronic Engineering,
BUET, Dhaka.

4. _____ 17.4.90 Member
(Dr. Mohammed Ali Choudhury)
Assistant Professor,
Department of Electrical and
Electronic Engineering,
BUET, Dhaka.

5. _____ Member
(Dr. Ahmed Shafi) (External)
Professor, Department of Physics,
University of Dhaka, Dhaka.

CERTIFICATE

This is to certify that this work has been done by me it has not been submitted elsewhere for the award of any degree or diploma.

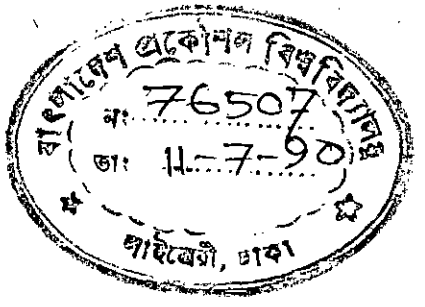

Countersigned

Signature of the student

(Dr. M. Rezwan Khan)

(Khwaja Mustafizur Rahman)

ACKNOWLEDGEMENT

The author expresses his sincere gratitude and profound respect to his supervisor Dr. M. Rezwan Khan, Associate Professor of Electrical and Electronic Engineering Department, BUET for his continuous guidance, constant encouragement and stimulating suggestions throughout the progress of this work.

The author also wishes to express his thanks and gratitude to Dr. Md. Abdul Matin, Professor and Head Department of Electrical and Electronic Engineering, BUET for his all-out support and encouragement to complete the work successfully.

The author acknowledges the help and support provided by his departmental colleagues. In particular he is indebted to Md. Monjurul Haque in connection with the preparation of the manuscript of this work.

The author finally is thankful to the Machine Dialogue Computer firm and to Tahsin Askar, Assistant Professor of Computer Science and Engineering Department, BUET for providing necessary support in some computational process of this work.

ABSTRACT

Potential channel structures having single and double discontinuities in lateral dimensions are studied in detail. A matrix formulation has been developed using the continuity conditions for the electron wave function and its derivative. It has been shown that the flow of current is very sensitive to the length and lateral dimensions of the channel segments. Significant variation of the channel width can be achieved by applying external voltage in the transverse direction which paves the way for the device to be used as an amplifier. Time response of the device is computed and is found to be very fast. Dependence of the current on the gate voltge is studied and the calculated results are presented. Values of the transconductance for the proposed amplifier are calculated and a relatively high value of transconductance comparable to that of the existing FETs are obtained.

CONTENTS

CHAPTER ONE

INTRODUCTION

INTRODUCTION

Quantum effects have started to play an important role in governing the behaviour of electronic devices, as the feature size of electronic devices shrink beyond the submicron level. The wave nature of electron must be taken into consideration while analyzing semiconductor structures, when characteristic dimensions are comparable to the mean free path of electrons. Prior to the development of modern thin film growth technology, it was impossible to obtain devices less than 3 μm in size, as at smaller sizes inaccuracies in the production of photomasks caused appreciable spread of geometrical dimensions and parameters of circuit elements. Now owing to a high resolution of optical device and photoresists it has become possible to prepare structures with dimensions of order of a few angstroms. The recent epitaxial growth techniques, particularly Molecular Beam Epitaxy (MBE), Metal-Organic Chemical Vapour Deposition (MOCVD) and Atomic Layer Epitaxy (ALE) has made it possible to fabricate ultrathin semiconductor layers that are smooth on an atomic scale.

1.1 LITERATURE REVIEW

Semiconductor microstructures such as metal-oxide-semiconductor, field effect transistor (MOSFET) and ultrathin p-n-p doping layers have provided researchers with a tool to study quasi-two-dimensional electronic systems [1,2]. The electrons are dynamically two dimensional in the sense that their motion is unrestricted in two spatial dimensions but quantized by a confining potential in the third dimension. The properties of electrons in such two dimensional structures have been studied extensively by Ando *et al.* [1]. In these experiments the microstructure is usually in the form of a channel which is terminated at opposite edges by uniformly doped regions in the semiconductor that serves as contacts. In the contact region the electrons' dynamical behaviour is bulk like. At the source end, a net current of carriers is injected from the central region into the channel; at the drain a net current is ejected from the channel. Both injection and ejection involve a change in the dynamical behaviour of the electron in two and three dimensional. Thin potential channel structure have been studied by a number of authors. Datta *et al.* [3] discussed a new configuration in which quantum interferences occur between two alternative paths provided by contiguous GaAs layers separated by an AlGaAs barrier layer. Alternatively, the conduction channels are defined lithographically on the surface of a FET-like structure. S. M. Fazlul Kabir [4] theoretically studied a similar structure, but much smaller in dimension. Two channels separated by a extremely thin potential barrier (15 Å) was considered. Gradual tunneling of electrons from one channel to the other was studied in detail and the variation of tunneling probabilities on the channel parameters was investigated. The problem of electron transport across a junction between two regions with very different

confining potential profiles in the transverse direction was first discussed by Kriman and Ruden [5]. A somewhat different method was presented by Frohne and Datta [6]. This method solves the problem by imposing boundary condition in some discrete points across the boundary. Waveguide discontinuity involving diaphragms, strip, change of guide cross section, change of propagation medium etc., deals with the similar type of mathematics. A number of such waveguide discontinuity problems are dealt elaborately by Lewin [7].

Ultrathin potential channel discontinuity problem studied in this thesis involves the similar type of mathematical approach presented by L. Lewin. This method takes the wave function at the interface as the unknown quantity and by imposing continuity conditions wave function at the interface is determined.

1.2 THESIS LAYOUT

Chapter 2 of this thesis deals with the method of analyzing the problem of electron propagation in ultra-thin potential structures, containing a discontinuity along the plane transverse to the direction of propagation.

Chapter 3 extends the method developed in chapter 2 to apply it to the potential structures containing double discontinuity. Numerous results are presented in chapter2 and chapter 3 applying the method developed, to some definite structures.

Possibility of using the structure is discussed in chapter 3 as high frequency amplifier is studied in chapter 4.

Chapter 5 presents the concluding discussions and recommendation for future works.

CHAPTER TWO

ANALYSIS OF POTENTIAL CHANNEL HAVING SINGLE DISCONTINUITY

2.1 INTRODUCTION

The problem of electron propagation in an ultrathin potential channel, discontinuous along a plane transverse to the direction of propagation is formulated in this chapter. A quantum treatment of the problem requires a knowledge of the spatial distribution of electron wave functions which can be obtained from solutions of the three dimensional Schrödinger equation. The solutions are subject to the continuity of the wavefunction and its derivative at the interfaces. Because of the wave nature of electrons, there is a non zero probability that electrons which are incident on the junction will be reflected. A semianalytic method has been developed to estimate the probability that the electrons are reflected by the junction, using the continuity of the wave function and its derivative at the interfaces. This method solves for the electron wave function at the discontinuity very accurately. A non-interacting single particle picture is adopted here while developing the model and the charge carriers are treated in the effective mass approximations. The effective mass is assumed to be constant throughout the channel. The restriction to a single mass is appropriate for doping structures in a homogeneous host material. The length of channel is considered to be smaller than the electron mean free path so that the phase coherence of the waves is not destroyed by scattering.

A channel structure having rectangular cross-section is analyzed by using the method developed in sec 2.2 and the calculated results are presented in sec 2.3.

2.2 GENERAL FORMULATION

A potential channel containing a discontinuity in the transverse plane is shown in figure (2.01). In the structure chosen, the direction of propagation is considered to be along the z direction. The interface, where the cross section of the potential channel changes abruptly is arbitrarily chosen at z = 0. At z=0, the channel potential is assumed to be discontinuous only along the x direction. The regions on the two sides of the discontinuity are labelled as I and II.

This is effectively a two dimensional electronic system in which motion of electrons is confined along the x direction and is unrestricted along the two other spatial directions. Now, the motion of electron in the potential structure is described by the time-independent Schrödinger equation [8]

$$H\Psi = E\Psi \qquad (2.01)$$

Where H is the Hamiltonian operator and E is the total energy of electron. This is an eigenvalue equation, with E representing the eigenvalue and Ψ the eigenfunction. The eigenvalue E is infinitely degenerate. Since the dependence of Ψ on y is not affected by the discontinuity in potential, we can, without any loss of generality, assume that $k_y = 0$. The wave equation (2.01) in each region then separates in the two space coordinates x and z

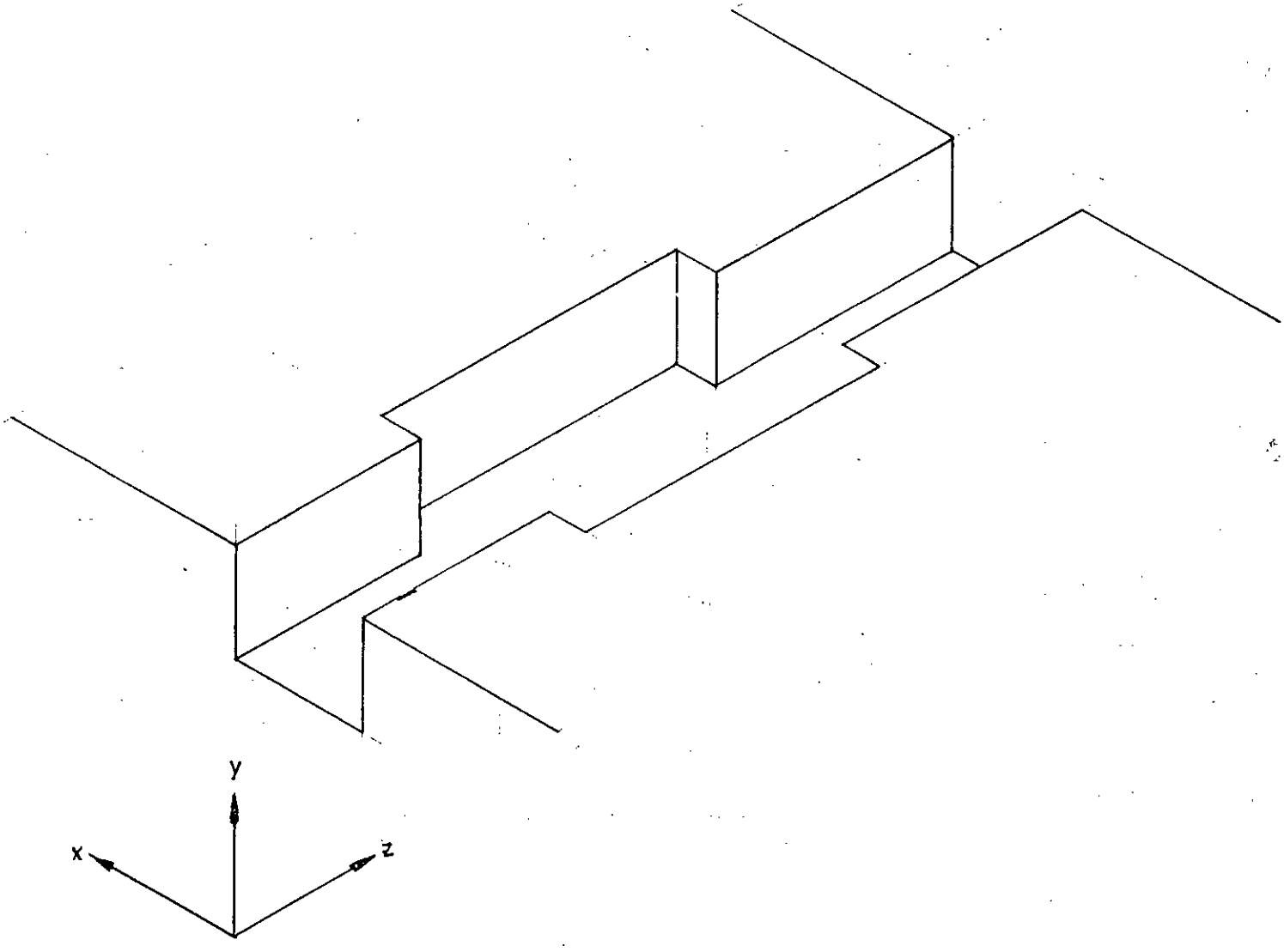

Figure (2.01). A potential channel discontinuous in the transverse plane.

$$\Psi(x,z)=\Psi(x)\Psi(z) \tag{2.02}$$

We further assume that the electron motion in the channel is restrained by perfectly rigid reflecting walls. Energy eigenfunctions $\Psi(x)$ are then characterized by discrete eigen values. Each of these eigenfunctions in region I represents a mode (or subband) in x. They are normalized and are orthonormal with each other, so that

$$\int_{-\infty}^{\infty}\Psi_{1p}(x)\Psi^{*}_{1q}(x)=0 \quad for \quad p=1,2,3.....$$
$$q=1,2,3.....$$
$$p\neq q$$
$$=1 \quad for \quad p=q \tag{2.03}$$

Here $\Psi 1n$ is the eigenfunction of the nth mode. As has been shown later, each of these eigenfunctions is characterized by a discrete energy level called the eigen energy of the particular mode. Now an arbitrary wave function $\Psi_I(x)$ in region I can be expanded in a series of these eigenfunctions as [9]

$$\Psi_l(x) = \sum_{n=1}^{\infty} c_n \Psi_{ln}(x)$$

(2.04)

The expansion coefficients c_n can be determined with the help of equation (2.03)

$$c_n = \int_{-\infty}^{\infty} \Psi_l(x) \Psi_{ln}^{*}(x) dx$$

(2.05)

The total energy of electron E is the sum of potential and kinetic energies. The potential energy of electron is constant throughout the structure and is taken without loss of generality to be zero. The total energy E can then be related to the wave vectors k_x and k_z, as

$$E = \frac{\hbar^2 k_x^2}{2m'} + \frac{\hbar^2 k_z^2}{2m'}$$

(2.06)

The assumption of constant potential energy is valid if the carrier density is uniform throughout the structure. Here, $\hbar$ is the modified planck's constant and m' is the effective mass of electron.

It is to be remembered that, E in equation (2.06) is the energy of electron

excluding the kinetic energy associate with motion along the y direction.

As mentioned earlier, the motion of electron is restricted in the x direction and corresponding energy assumes discrete values, with each value characterizing a particular mode. This discrete energy level which characterizes a particular mode is called the eigen energy of that mode. The fundamental mode has the lowest value of eigen energy and eigen energy of higher modes goes on increasing in discrete levels. If we define the eigen energy of the nth mode as E_{1n}, then the wave vector in the z direction for the nth mode can be obtained from relation (2.06)

$$k_{z1n} = \frac{\sqrt{2m^*(E - E_{1n})}}{\hbar} \qquad (2.07)$$

From now on suffix z will not be used to represent the wave vector in the z direction, so that k_{1n} will simply mean the wave vector of the nth mode in the z direction.

If the eigen energy of a particular mode is less than the electron energy E then, we see from equation (2.07) that the mode will have real wave vector k_z and will be propagating in nature. But if the eigen energy is greater than the electron energy, then the wave vector will be imaginary and the mode will be decaying in nature.

Like the wave function $\Psi_I(x)$, the wave function $\Psi_{II}(x)$ in region II, can be expressed as a summation of infinite number of orthonormal eigenfunction, with each eigenfunction representing a particular mode (or subband)

$$\Psi_{II}(x) = \sum_{n=1}^{\infty} a_n \Psi_{2n}(x)$$

(2.08)

Where, as before, all the eigenfunctions are normalized and are orthonormal to each other so that

$$\int_{-\infty}^{\infty} \Psi_{2p}(x)\Psi_{2q}^{*}(x) = 0 \quad for \quad p = 1, 2, 3.....$$

$$q = 1, 2, 3.....$$

$$p \neq q$$

$$= 1 \quad for \quad p = q$$

(2.09)

The propagation vector in region II can be expressed by a similar relation as (2.07)

$$k_{2n} = \frac{\sqrt{2m^{*}(E - E_{2n})}}{\hbar}$$

(2.10)

where, E_{2n} is the eigen energy of the nth mode in region II.

Let us consider an electron of a particular subband (mode) incident on the junction from the left with energy E. Because of the need to match both wave functions and its derivative at the junction, it will give rise to reflected and transmitted waves, in all the different subbands. The number of propagating modes (including the incident mode), that the reflected waves contain, depends on the total electron energy E and the eigen energies of the different modes. Those modes will be propagating in nature for which the electron energy is greater than the corresponding eigen energy and the rest of the modes for which the electron energy is less than the eigen energy will be decaying in nature. Far from the junction the effect of the decaying modes die out, but they must be taken into account in order to satisfy the boundary conditions at the junctions between regions I and II. The total wave function in region I, can be written in context to the relation (2.04) and the foregoing analysis, as

$$\Psi_1(x,z) = \Psi_{1p}(x)e^{-jk_{1p}z} + \sum_{q=1}^{\infty} \lambda_{qp}\Psi_{1q}(x)e^{jk_{1q}z} \qquad (2.11)$$

Here, the first term is representing the incident wave of a particular mode p. The second term is representing the sum of all the reflected (decaying and propagating) modes. λ_{qp} is the reflection amplitude of a particular mode q generated from the incident mode p. k's are the wave vectors given by the relation (2.07). As mentioned earlier, the wave vectors k along the z direction

for the evanescent modes are imaginary. It is also important to choose the proper sign of the imaginary wave vectors in equation (2.11) so that the wave functions decay exponentially from the junction at z = 0.

Region II contains transmitted waves only, so that the wave function for region II can be written as

$$\Psi_{II}(x,z)=\sum_{q'=1}^{\infty} T_{q'p}\Psi_{2q'}(x)e^{-jk_{2q'}z} \tag{2.12}$$

Region II contains no discontinuity to its right so that there are no reflected waves in region II. Here, $T_{q'p}$ is the transmission amplitude of the qth mode of region II generated by the incident pth mode in region I. $k_{2q'}$ is the wave vector of the $q'th$ mode for region II given by the equation (2.10). $k_{2q'}$ is imaginary for those modes which are nonpropagating. As in region I, proper sign for these imaginary wave vectors should be chosen in equation (2.12) so that their corresponding modes decay exponentially from the junction.

The continuity of the wave function Ψ at the interface gives us

$$\Psi_{1p}(x)+\sum_{q=1}^{\infty}\lambda_{qp}\Psi_{1q}(x)=\sum_{q'=1}^{\infty} T_{q'p}\Psi_{2q'}(x) \tag{2.13}$$

Now multiplying both sides by $\Psi_{2q'}(x)$ and integrating with the help of equation (2.09) we obtain

$$T_{q'p} = \int_{-\infty}^{\infty} \Psi_{1p}(x)\Psi^{*}_{2q'}(x)dx + \sum_{q=1}^{\infty} \lambda_{qp} \int_{-\infty}^{\infty} \Psi_{1q'}(x)\Psi^{*}_{2q'}(x)dx$$

$$= A_{pq'} + \sum_{q=1}^{\infty} \lambda_{qp} A_{qq'} \qquad (2.14)$$

where

$$A_{mn} = \int_{-\infty}^{\infty} \Psi_{1m}(x)\Psi^{*}_{2n}(x)dx \qquad (2.15)$$

The derivative $(\partial\Psi/\partial z)$ in region I and II, respectively are given by

$$\frac{\partial \Psi_{I}}{\partial z} = -jk_{1p}\Psi_{1p}(x)e^{-jk_{1p}z} + j\sum_{q=1}^{\infty} k_{1q}\lambda_{qp}\Psi_{1q}(x)e^{jk_{1q}z} \qquad (2.16)$$

and

$$\frac{\partial \Psi_{II}}{\partial z} = -j\sum_{q'=1}^{\infty} k_{2q'}T_{q'p}\Psi_{2q'}(x)e^{-jk_{2q'}z} \qquad (2.17)$$

By imposing continuity condition on $\partial\Psi/\partial z$ at z=0 by using equation (2.14) we obtain

$$-jk_{1p}\Psi_{1p}(x)+j\sum_{q=1}^{\infty}k_{1q}\lambda_{qp}\Psi_{1q}(x)$$

$$=-j\sum_{q'=1}^{\infty}k_{2q'}\Psi_{2q'}(x)\left[A_{pq'}+\sum_{q=1}^{\infty}\lambda_{qp}A_{qq'}\right]$$

(2.18)

To hold the above equality, all modal components of the Ψ_{I}' function in equation (2.18) must coincide with the corresponding modal components of the Ψ_{II}' function.

equating the component of the incident mode $\Psi_{1p}(x)$ from equation (2.18) and rearranging we have

$$\lambda_{1p}\left[j\sum_{q'=1}^{\infty}k_{2q'}A_{1q'}A_{pq'}\right]+\lambda_{2p}\left[j\sum_{q'=1}^{\infty}k_{2q'}A_{2q'}A_{pq'}\right]$$

$$+\lambda_{3p}\left[j\sum_{q'=1}^{\infty}k_{2q'}A_{3q'}A_{pq'}\right]+\ldots\ldots\ldots\ldots$$

$$+\lambda_{pp}\left[jk_{1p}+j\sum_{q'=1}^{\infty}k_{2q'}A_{pq'}^{2}\right]+\ldots\ldots\ldots\ldots$$

$$=jk_{1p}-j\sum_{q'=1}^{\infty}k_{2q'}A_{pq'}^{2}$$

(2.19)

Equating the component of any arbitrary nth mode $(\Psi_{1n}(x))$, when the selected mode is not the incident mode we have

$$\lambda_{1p}\left[j\sum_{q'=1}^{\infty} k_{2q'} A_{1q'} A_{nq'} \right] + \lambda_{2p}\left[j\sum_{q'=1}^{\infty} k_{2q'} A_{2q'} A_{nq'} \right]$$

$$+ \lambda_{3p}\left[j\sum_{q'=1}^{\infty} k_{2q'} A_{3q'} A_{nq'} \right] + \cdots\cdots\cdots$$

$$+ \lambda_{np}\left[jk_{1n} + j\sum_{q'=1}^{\infty} k_{2q'} A_{nq'}^{2} \right] + \cdots\cdots\cdots$$

$$= -j\sum_{q'=1}^{\infty} k_{2q'} A_{nq'} A_{pq'} \qquad (2.20)$$

Our objective is to determine the reflection amplitude λs. In order to satisfy the boundary condition at every point at the junction we require infinite number of modes to be considered and by equating the modal components from equation (2.18) we will have infinite number of equations to solve the infinite number of unknown λs. But to solve the problem numerically (on a computer) we must limit the number of modes and it will be shown later in this chapter, that, if we consider just a few decaying modes in addition to the propagating mode we will be able to predict the nature of the Ψ function at the interface with reasonable accuracy.

If n modes are considered we will have n equations by equating individual modal components from equation (2.18). Solving the equations n number of reflection amplitudes can be determined. In matrix form we can write these equations as

$$\begin{bmatrix} B_{11} & B_{12} & B_{13} & . & . & . & B_{1n} \\ B_{21} & B_{22} & B_{23} & . & . & . & B_{2n} \\ . & . & . & . & . & . & . \\ B_{p1} & B_{p2} & B_{p3} & . & B_{pp} & . & B_{pn} \\ . & . & . & . & . & . & . \\ B_{n1} & B_{n2} & B_{n3} & . & . & . & B_{nn} \end{bmatrix} \begin{bmatrix} \lambda_{1p} \\ \lambda_{2p} \\ . \\ . \\ . \\ \lambda_{np} \end{bmatrix} = \begin{bmatrix} C_{11} \\ C_{21} \\ . \\ . \\ . \\ C_{n1} \end{bmatrix}$$

where

$$B_{\alpha\alpha} = jk_{1\alpha} + j\sum_{n=1}^{\infty} k_{2n} A_{\alpha n}^2$$

$$\alpha = 1, 2, 3.....$$

(2.21)

$$B_{\alpha\beta} = B_{\beta\alpha} = j\sum_{n=1}^{\infty} k_{2n} A_{\alpha n} A_{\beta n}$$

$$\alpha = 1, 2, 3.....$$

$$\beta = 1, 2, 3.....$$

$$\alpha \neq \beta$$

(2.22)

$$C_{p1} = jk_{1p} - j\sum_{n=1}^{\infty} k_{2n} A_{pn}^2$$

(2.23)

$$C_{\alpha l} = -j \sum_{n=1}^{\infty} k_{2n} A_{pn} A_{\alpha n}$$

$$\alpha = 1, 2, 3 \ldots\ldots$$

$$\alpha \neq p$$

(2.24)

2.3 RESULTS AND DISCUSSION

An illustrative result is presented in this section by applying the method developed in section 2.2 to a definite potential structure containing discontinuity in the transverse direction. Throughout the calculation infinite potential wall is assumed so that electron wave function Ψ vanishes outside the channel. Although the calculation is made on the basis of infinite barrier, the method is applicable if the potential wall is finite. But in such case the overlapping constants A's are to be calculated numerically.

We consider a simple structure of rectangular section, as shown in the figure 2.2. Since infinite potential barrier is assumed, the normalized wave function $\Psi(x)$ in the two regions can be written as

$$\Psi_{1n}(x) = \sqrt{\frac{2}{a}} \sin \frac{n\pi x}{a} \qquad for\ x < a$$

$$= 0 \qquad for\ x \geq a$$

(2.25)

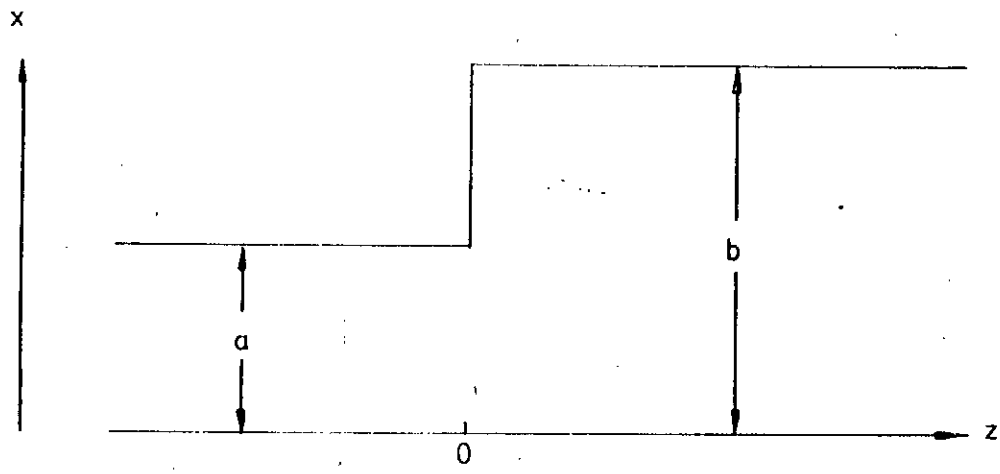

Figure (2.02). Transverse dimensions of a potential channel discontinuous at the plane z=0. The channel cross-section is rectangular throughout the structure.

$$\Psi_{2n}(x) = \sqrt{\frac{2}{b}} \sin \frac{n\pi x}{b} \qquad for\ x < b$$

$$= 0 \qquad for\ x \geq b \tag{2.26}$$

where

$$E_{1n} = \frac{\hbar^2 n^2 \pi^2}{2m^* a^2}$$

and

$$E_{2n} = \frac{\hbar^2 n^2 \pi^2}{2m^* b^2}$$

Here a and b are the transverse dimensions of region I and II respectively.

Calculation of the overlapping constants A_{mn}, defined by the relation (2.15) is shown in Appendix B

In our calculation we have considered the transverse dimension 'b' of the second region to be 100 Å, energy of electron E to be 140 mev and effective mass $m^* = 0.1 m_o$, where m_o is the free mass of electron. The transverse dimension of the first region 'a' is varied from 52 Å to 100 Å. Energy of electron is chosen in a way such that only the fundamental mode can propagate in the two regions. Using the method developed in section 2.2 the variation of the reflection and the transmission amplitude of the propagating mode with 'a' are calculated and is shown in the fig (2.3). We see from the

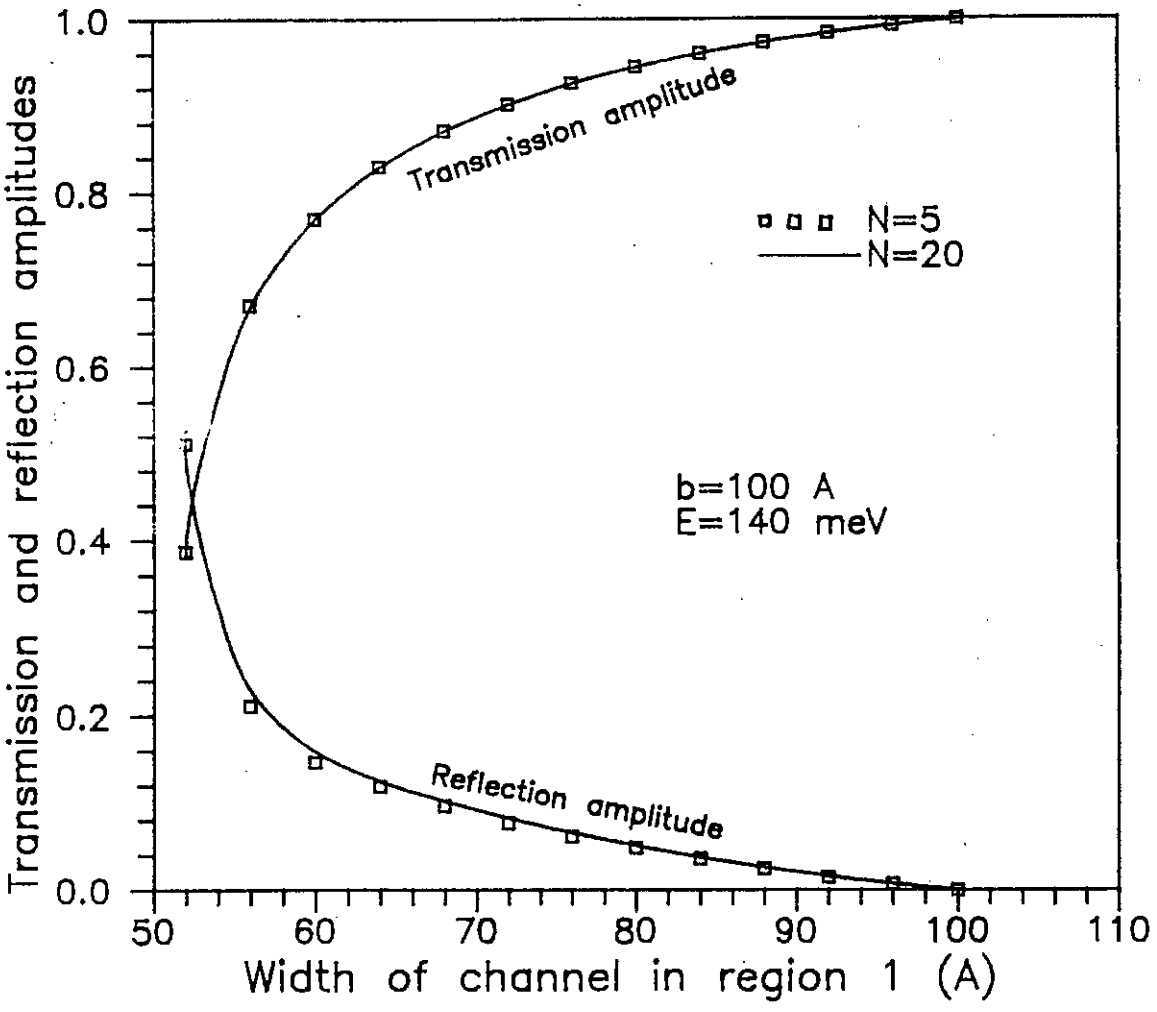

Figure (2.03). Transmission and Reflection amplitudes as functions of channel width in region I for an electron energy of 140 meV.

figure, reflection becomes zero when the channel contains no discontinuity (a = 100 Å). Reflection and transmission amplitude are calculated for n = 5 and 20, where n is the number of modes (including the propagating mode), those are considered while calculating the two amplitudes. It is found that n=5 gives a reasonably good result. So we observe though infinite number of modes are required to be considered to satisfy the boundary conditions, only a few mode can give quite accurate result.

CHAPTER THREE

ANALYSIS OF POTENTIAL CHANNEL HAVING DOUBLE DISCONTINUITY

3.1 INTRODUCTION:

The problem of electron propagation in a potential structure having double discontinuities is analyzed in this chapter. First a mathematical model is developed extending the solution technique presented in chapter 2 then some results are presented for different channel structures having double discontinuities.

3.2 MATHEMATICAL FORMULATION:

Let us consider two abrupt junction in a potential microstructure between three regions I, II and III of dissimilar transverse width as shown in figure (3.01). The motion of electron in the structure is bounded along the x direction by potential barriers but is unrestricted along the two other spatial directions y and z. The direction of propagation is considered along the z direction only. Region II of the structure is of finite length l but the two other regions are of semi-infinite in extent along the direction of propagation. The discontinuities are chosen at z=0 and at z=l.

The electron wave function $\Psi(x)$ has different distributions at the three regions I, II and III. In order to match the electron wave function and its derivatives at the two interfaces infinite number of modes are needed to be considered at each junction. Some of these modes are propagating and the

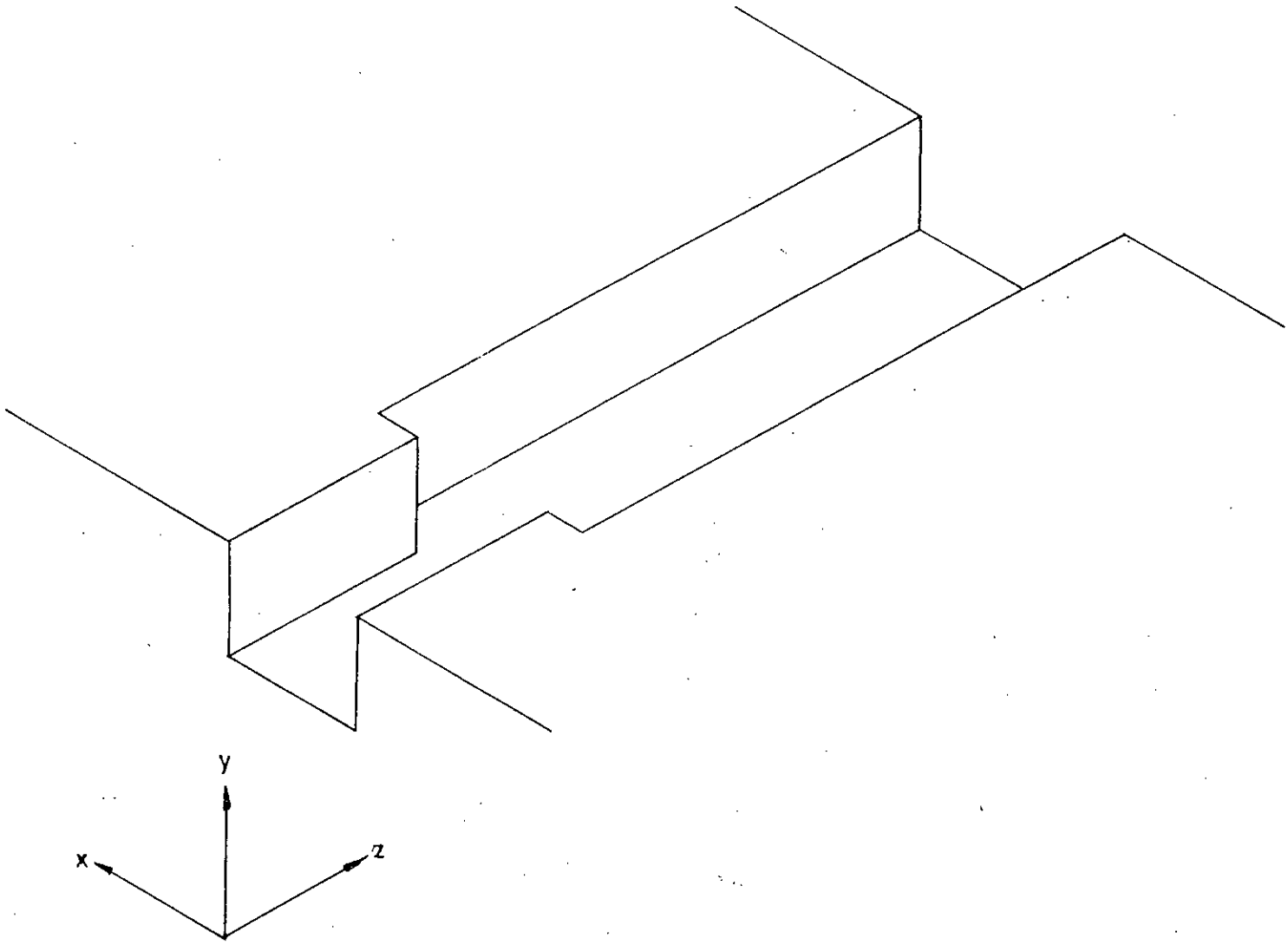

Figure (3.01). A potential channel having double discontinuities in the transverse plane.

rest are attenuating. Though the effect of the attenuating modes die out with distance from the junction, their effect is significant near the junction.

The method for solving single junction channel problem presented in the previous chapter, is extended here to solve the wave functions in all the three regions. The wave functions at the respective regions are written in terms of their decaying and propagating modes, the continuity conditions are then imposed in order to determine the reflection and transmission amplitudes for each region. The assumptions made for single junction channel problem are also valid for our present analysis.

Let an electron of a particular mode α incidents the junction at z=0 from left, the incident electron gives rise to reflected wave in all the different subbands, so the total wave function Ψ for region I can be written in terms of the reflected and the incident waves as

$$\Psi_I(x,z) = \Psi_{1\alpha}(x)e^{-jk_{1\alpha}z} + \sum_{\beta=1}^{\infty} \lambda_{\beta\alpha}\Psi_{1\beta}(x)e^{jk_{1\beta}z} \qquad (3.01)$$

where $\lambda_{\beta\alpha}$ is the reflection amplitude of mode β generated from the incident mode α, the k's are wave vectors and are imaginary for those modes which are decaying, $\Psi_{1\beta}$ are the eigenfunctions for region I, they are normalized and are orthonormal with each other.

In a similar manner the transmitted wave in region II from region I contains propagating and decaying modes. The number of modes that propagate in region II depends on the energy of electron E and the eigen energies of the region. Region II not only contains these transmitted modes travelling in the positive z direction but also contains propagating and decaying modes in the negative z direction. These second set of modes have been generated by the first set of modes when they are incident at the junction. The decaying modes in region II generated at each junction will be able to reach the other junction before dying out, if the intermediate region length l is not large enough. So their effect must be considered in both the junctions.

The total wave function at region II can be expressed in terms of these transmitted and reflected waves as

$$\Psi_{II}(x,z)=\sum_{y=1}^{\infty} T_{2y}\Psi_{2y}(x)e^{-jk_{2y}z}+\sum_{y=1}^{\infty} R_{2y}\Psi_{2y}(x)e^{-jk_{2y}(l-z)} \qquad (3.02)$$

here $T_{2\gamma}$ is the transmission amplitude of the γth mode at junction 1 and $R_{2\gamma}$ is the reflection amplitude of the mode at junction 2. $K_{2\gamma}$ is the wave vector for the γth mode at region II and it is imaginary if the mode is nonpropagating. The nonpropagating modes in region II are of greater importance since they can significantly contribute to the current flow (appendix A).

The total wave function for region III can be written as

$$\Psi_{III}(x,z) = \sum_{\delta=1}^{\infty} T_{3\delta}\Psi_{3\delta}(x)e^{-jk_{3\delta}(z-l)} \qquad (3.03)$$

Region III has no discontinuity to its right, so Ψ_{III} contains no reflected wave. Here $T_{3\delta}$ is the transmission amplitude of the mode δ, at the junction 2.

To determine the reflection and the transmission amplitudes we impose the boundary conditions at the two interfaces. We first apply the continuity condition for the wave function at the two junctions

Applying the continuity condition for function Ψ at z=0 we have

$$\Psi_I(x,z) = \Psi_{II}(x,z)$$

(3.04)

or

$$\Psi_{1\alpha}(x) + \sum_{\beta=1}^{\infty} \lambda_{\beta\alpha} \Psi_{1\beta}(x) = \sum_{\gamma=1}^{\infty} T_{2\gamma} \Psi_{2\gamma}(x) + \sum_{\gamma=1}^{\infty} R_{2\gamma} \Psi_{2\gamma}(x) e^{-jk_{2\gamma} l}$$

(3.05)

From continuity of Ψ at junction 2 (z=l) we have

$$\Psi_{II}(x,z) = \Psi_{III}(x,z)$$

(3.06)

or

$$\sum_{\gamma=1}^{\infty} T_{2\gamma} \Psi_{2\gamma}(x) e^{-jk_{2\gamma} l} + \sum_{\gamma=1}^{\infty} R_{2\gamma} \Psi_{2\gamma}(x) = \sum_{\delta=1}^{\infty} T_{3\gamma} \Psi_{3\gamma}(x)$$

(3.07)

Multiplying both sides of the of equation ((3.05) by $\Psi^*_{2\gamma}(x)$ and integrating, we get

$$T_{2y} + R_{2y} e^{-jk_{2y}l} = \int_{-\infty}^{\infty} \Psi_{1a}(x) \Psi^{*}_{2y}(x) dx + \sum_{\beta=1}^{\infty} \lambda_{\beta a} \int_{-\infty}^{\infty} \Psi_{1\beta}(x) \Psi^{*}_{2y}(x) dx$$

(3.08)

or

$$T_{2y} + R_{2y} e^{-jk_{2y}l} = A_{ay} + \sum_{\beta=1}^{\infty} \lambda_{\beta a} A_{\beta y}$$

(3.09)

where

$$A_{mn} = \int_{-\infty}^{\infty} \Psi_{1m}(x) \Psi^{*}_{2n}(x) dx$$

$$m = 1, 2, 3.....$$

$$n = 1, 2, 3.....$$

(3.10)

Similarly from equation (3.07), we can get

$$T_{2y} e^{-jk_{2y}l} + R_{2y} = \sum_{\delta=1}^{\infty} T_{3\delta} \int_{-\infty}^{\infty} \Psi_{3\delta}(x) \Psi^{*}_{2y}(x) dx$$

(3.11)

or

$$T_{2\gamma}e^{-jk_{2\gamma}l} + R_{2\gamma} = \sum_{\delta=1}^{\infty} T_{3\delta}B_{\delta\gamma} \qquad (3.12)$$

where

$$B_{mn} = \int_{-\infty}^{\infty} \Psi_{3m}(x)\Psi_{2n}^{*}(x)dx$$

$$m = 1, 2, 3.....$$

$$n = 1, 2, 3..... \qquad (3.13)$$

We next apply the continuity of the function $\partial\Psi/\partial z$ at the respective junctions

Applying to junction 1 at z=0 we have

$$\frac{\partial\Psi_{I}(x,z)}{\partial z} = \frac{\partial\Psi_{II}(x,z)}{\partial z} \qquad (3.14)$$

or

$$-jk_{1\alpha}\Psi_{1\alpha}(x)+j\sum_{\beta=1}^{\infty}k_{1\beta}\lambda_{\beta\alpha}\Psi_{1\beta}(x)$$

$$=-j\sum_{\gamma=1}^{\infty}k_{2\gamma}T_{2\gamma}\Psi_{2\gamma}(x)+j\sum_{\gamma=1}^{\infty}k_{2\gamma}R_{2\gamma}\Psi_{2\gamma}(x)e^{-jk_{2\gamma}l} \tag{3.15}$$

Equating the modal component of the incident mode from equation (3.15) and rearranging we have

$$j\sum_{\gamma=1}^{\infty}k_{2\gamma}T_{2\gamma}A_{\alpha\gamma}-j\sum_{\gamma=1}^{\infty}R_{2\gamma}K_{2\gamma}A_{\alpha\gamma}e^{-jk_{2\gamma}l}+$$

$$jk_{1\alpha}\lambda_{\alpha\alpha}=jk_{1\alpha} \tag{3.16}$$

Equating the component of any arbitrary mode Ψ_{1n} from equation (3.15) when the selected mode is not the incident mode we have

$$j\sum_{\gamma=1}^{\infty}k_{2\gamma}T_{2\gamma}A_{n\gamma}-j\sum_{\gamma=1}^{\infty}K_{2\gamma}R_{2\gamma}A_{n\gamma}e^{-jk_{2\gamma}l}+jk_{1n}\lambda_{n\alpha}=0 \tag{3.17}$$

Next applying to junction 2 at z=l and using equation (3.2) and (3.3) we have

$$\frac{\partial \Psi_{II}(x,z)}{\partial z} = \frac{\partial \Psi_{III}(x,z)}{\partial z} \tag{3.18}$$

or

$$-j\sum_{\gamma=1}^{\infty} k_{2\gamma} T_{2\gamma} \Psi_{2\gamma}(x) e^{-jk_{3\gamma} l} + j\sum_{\gamma=1}^{\infty} k_{2\gamma} R_{2\gamma} \Psi_{2\gamma}(x) = -j\sum_{\delta=1}^{\infty} k_{3\delta} T_{3\delta} \Psi_{3\delta}(x) \tag{3.19}$$

Equating any arbitrary mth mode (Ψ_{3m}) from equation (3.19) we have

$$j\sum_{\gamma=1}^{\infty} k_{2\gamma} T_{2\gamma} B_{m\gamma} e^{-jk_{2\gamma} l} - j\sum_{\gamma=1}^{\infty} k_{2\gamma} R_{2\gamma} B_{m\gamma} - jk_{3m} T_{3m} = 0 \tag{3.20}$$

where the constants A_{mn} and B_{mn} are defined earlier.

The boundary condition must be met at every point along the two interfaces and this is only possible if we include an infinite number of modes in all the three regions. But to solve the problem numerically on a computer, we limit the modes to a reasonable number n as we have done for single junction. If we consider n modes, we have to solve for the n reflection amplitudes for

region I, n transmission and n reflection constants for region II and n transmission constants for region III. So we require 4n simultaneous independent equations to solve these 4n unknowns. Out of these 4n equations, 2n number of equations can be obtained by equating the modal components at the two junctions from equations (3.15) and (3.17) and the other 2n number of equations can be obtained from the overlapping integral equations (3.09) and (3.11). So the number of unknowns match with the number of equations, hence the 4n unknowns can be solved by solving the 4n equations.

3.3 RESULTS

The solution technique presented in section (3.2) is applied to some potential structures to observe the effect of varying channel dimensions on the current flow. Rectangular structures with infinite potential barrier are assumed throughout. Effective mass of electron is taken to be $0.1m_o$, where m_o is the free electron mass. The structure is shown in figure (3.02) where 'a' and 'c' are the width of region I and III respectively, b and l are the width and length of region II.

3.3.1 EFFECT OF VARYING LENGTH OF REGION II

We first observe the effect of varying the length l on current, transmission and reflection amplitudes.

STRUCTURE SYMMETRICAL ABOUT THE CHANNEL AXIS:

A structure is considered which is symmetrical about the channel axis as shown in figure (3.03). The transverse dimensions are, 80 Å for region I, 140 Å for region II and 80 Å for region III. Electron energy is chosen to be 100 meV. Calculations are made for the reflection and transmission constants of the first and the third region respectively, for the first four modes and are shown in the figure (3.04), the even modes are found to be absent which is

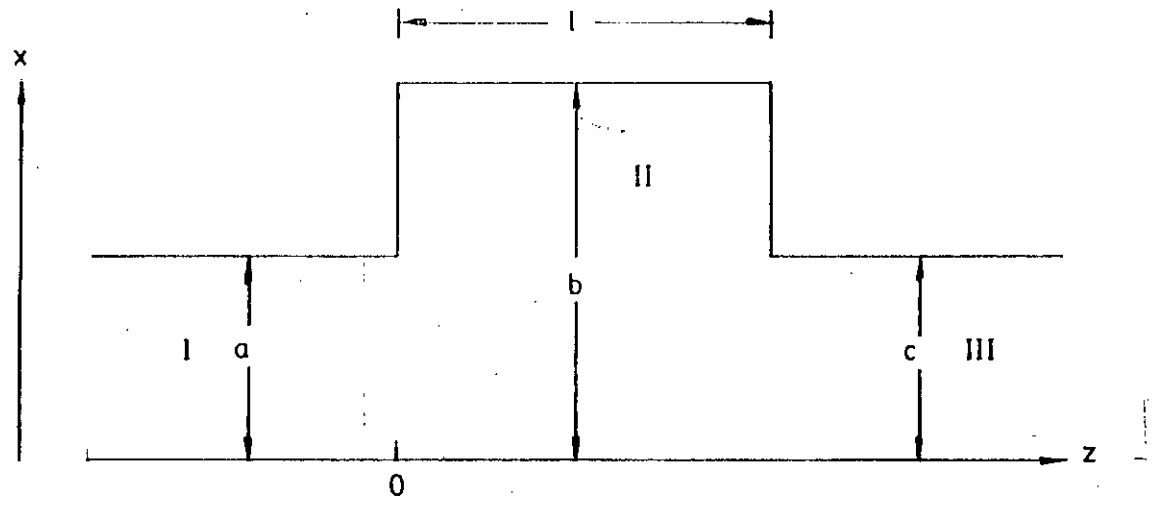

Figure (3.02). Top view of a potential channel having double discontinuities in the transverse plane. The channel cross-section is rectangular throughout the structure.

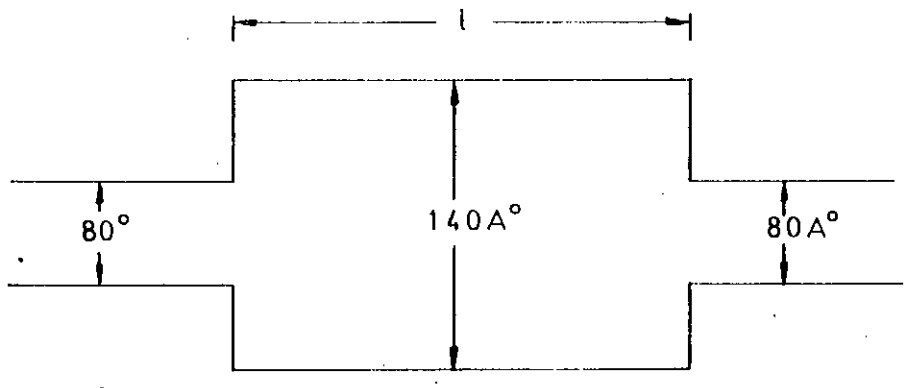

Figure (3.03). Transverse dimensions of a potential channel with double discontinuities in the transverse plane. The channel cross-section throughout the structure is rectangular and is symmetrical about the channel axis.

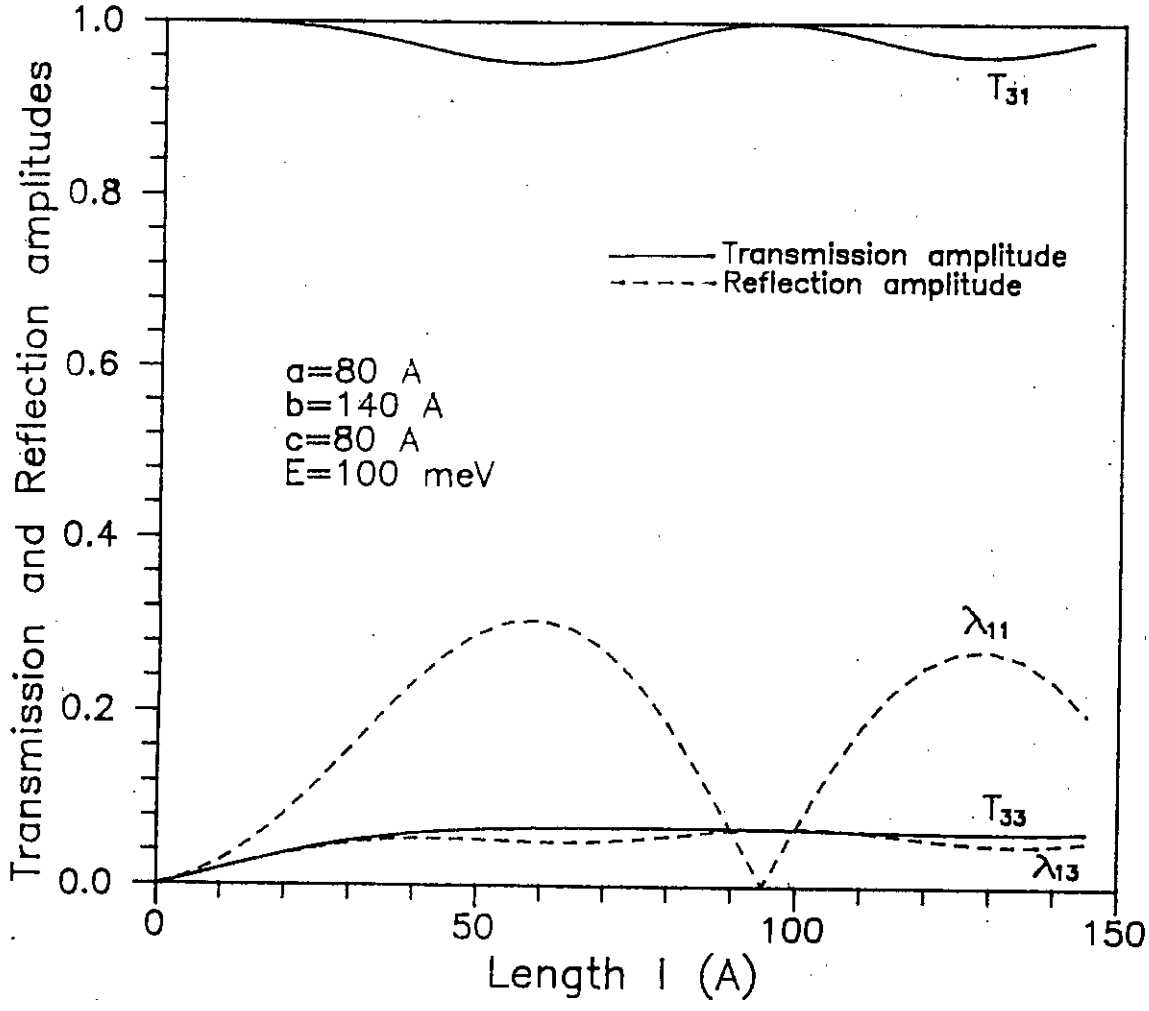

Figure (3.04). Transmission and Reflection amplitudes as functions of channel length in region II for an electron energy of 100 meV.

expected due to the symmetry of the structure. For the chosen energy and dimensions only the fundamental mode in the respective two regions is propagating, the other modes are attenuating in nature.

CURRENT IN THE STRUCTURE FOR TWO DIFFERENT ENERGIES:

The variation of current with length l in the structure is claculated and is shown in figure (3.05) and (3.06) for two different energies, 100 meV and 200 meV respectively. We can see from the figures that current for 100 meV shows slight variation with l, whereas the current for 200 meV varies sharply with l. At 100 mev only one propagating mode can exist in region II. On the other hand two propagating modes (1st and 3rd) can exist at region II when electron energy is 200 meV. Owing to the difference in wave vectors k, the phase difference of these two modes change continuously with distance. Depending on length l they interfere constructively or destructively producing the observed variation of current. For 100 meV there exists only one propagating mode in region II and therefore no sharp variation of current is observed. It is worth mentioning that the shape of these curves are not only defined by the propagating modes; decaying modes can also contribute significantly to the current. Moreover amplitude and phase of the propagating modes are different for different length l, which results in a complex variation of current.

The variation of the reflection and transmission amplitude in the intermediate region are also shown in figure (3.07), for electron energy of 200 meV.

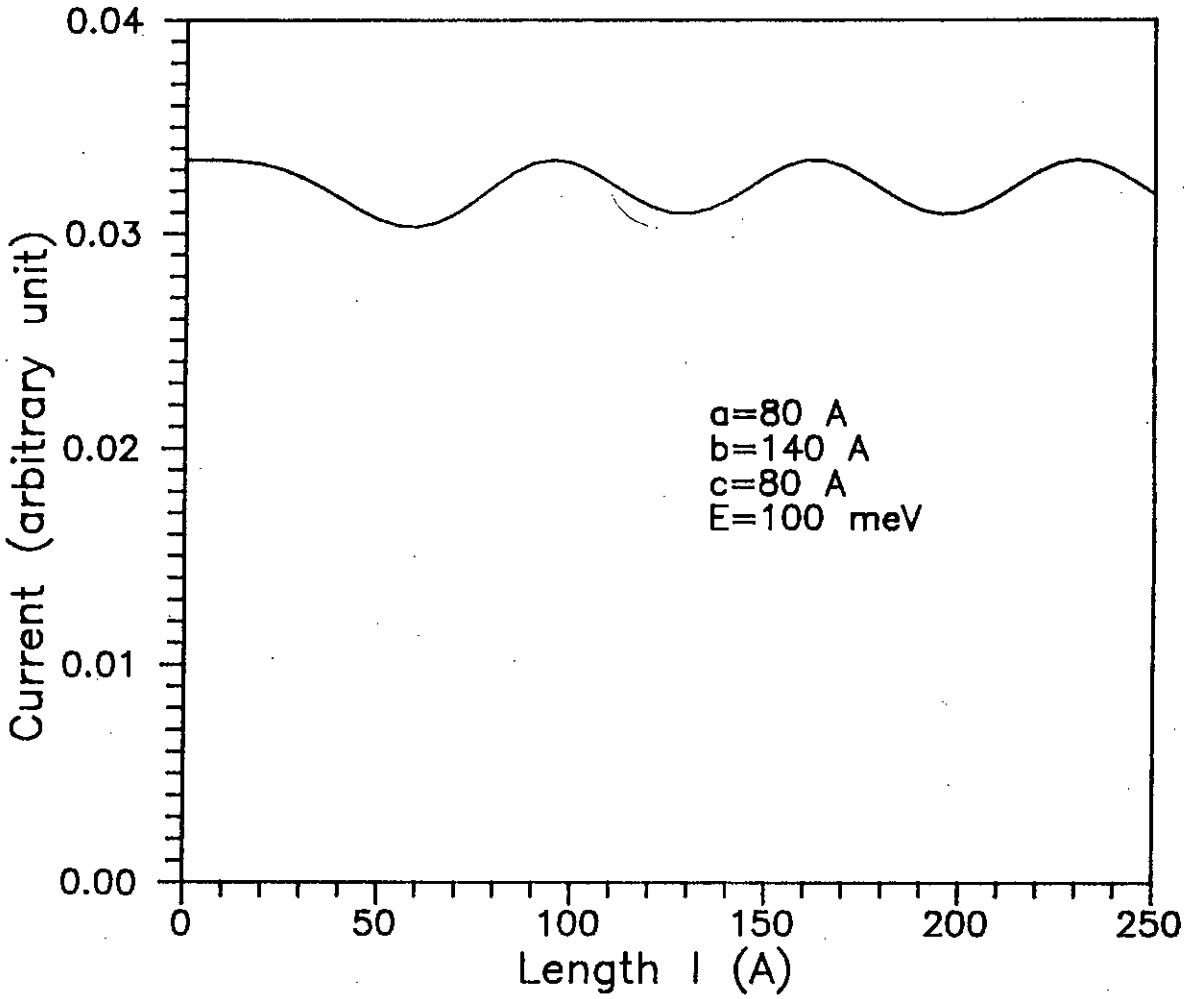

Figure (3.05). A plot of current versus channel length in region II for an electron energy of 100 meV.

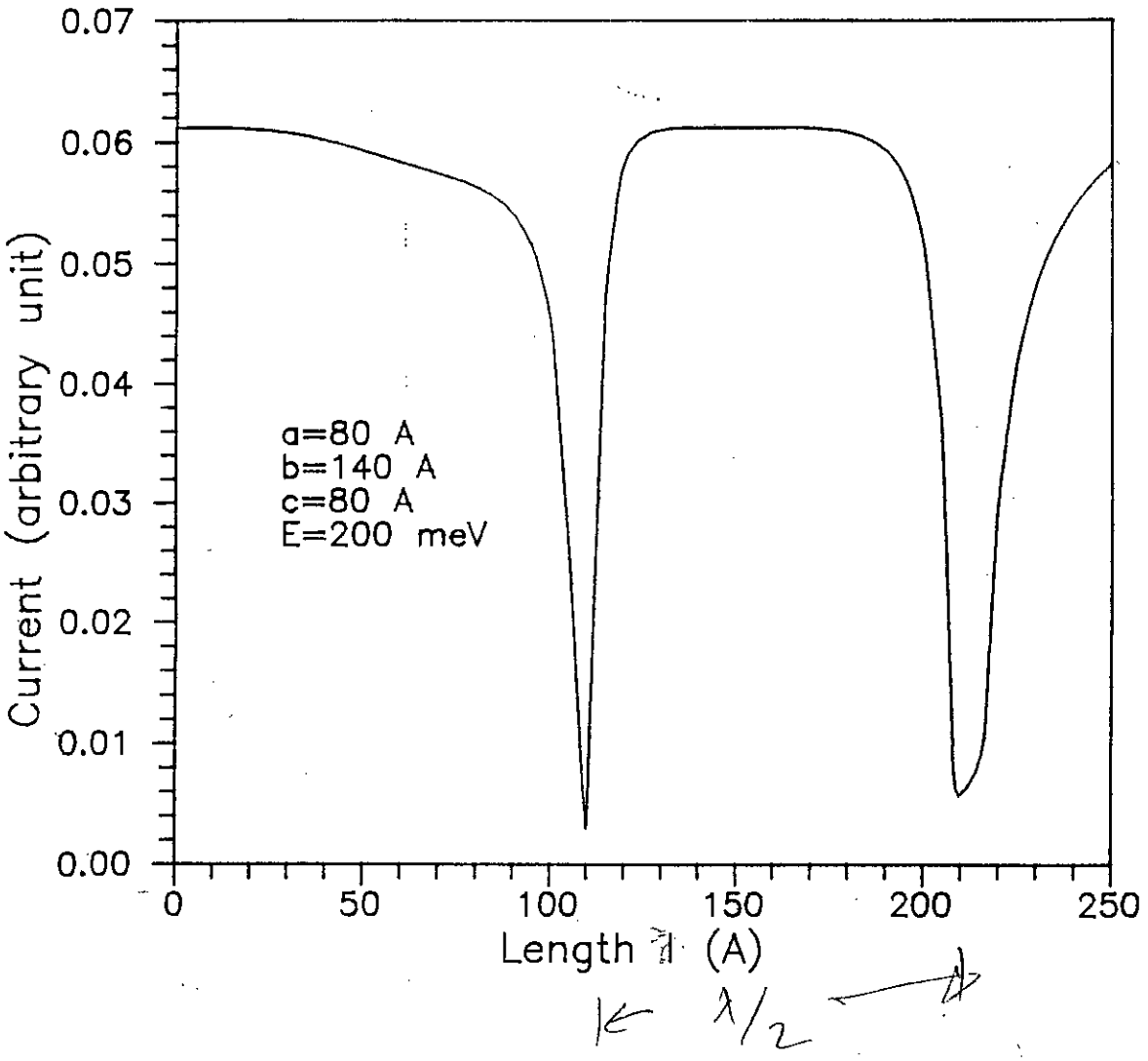

Figure (3.06). A plot of current versus channel length in region II for an electron energy of 200 meV.

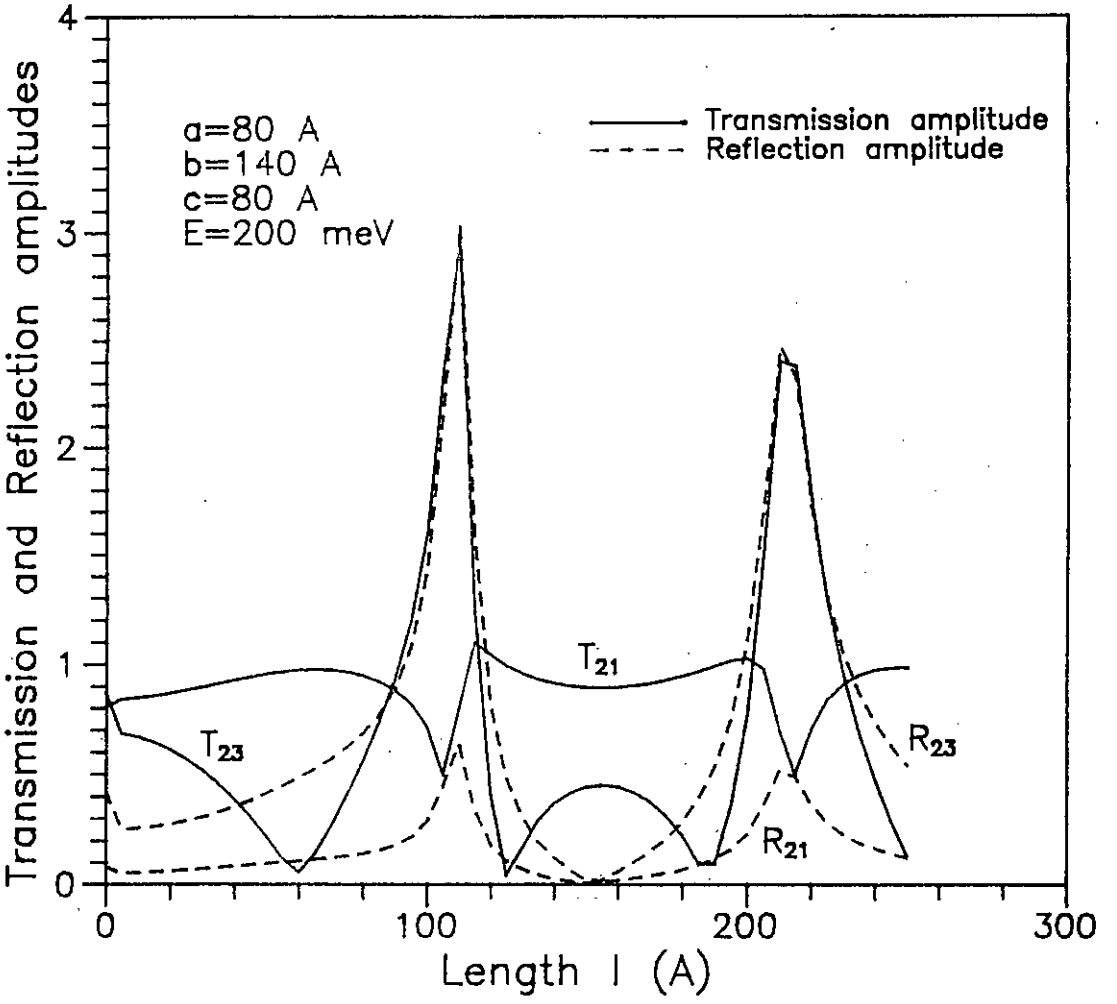

Figure (3.07). Transmission and Reflection amplitudes as functions of channel length in region II for an electron energy of 200 meV.

We next choose a structure with a=80 Å, b=140 Å and c=80 Å. Energy E is chosen to be 100 meV. The variation of the reflection amplitude of the first region and the transmission amplitude of the third region, with variation of length l is calculated and is presented in figure (3.08). We can see from the figure that for l=0, reflection is 0 and transmission is 1. This is expected since for l=0 the structure possesses no discontinuity. With the increase of length l, reflection increases and transmission decreases. The reflection and transmission amplitudes shown in the figure are of the fundamental mode, the only propagating mode in the two regions I and II.

3.3.2 EFFECT OF VARYING THE WIDTH OF IST REGION

The effect of varying the width of region I is studied in this section. We first choose a structure with l=350 Å, b=300 Å and c=90 Å (fig 3.02). Variation of current for three different energies with a is shown in figure (3.09). A random variation of current for different energies are observed in the figure. Decreasing the length and width of region II to 125 Å and 175 Å respectively, a smooth variation of current is obtained as shown in figure (3.10), a similarity in the shape of the curves for different energies is also observed in the figure. From the results obtained in this section we can conclude, a smooth variation of current can be obtained by an effective choice of the channel dimensions.

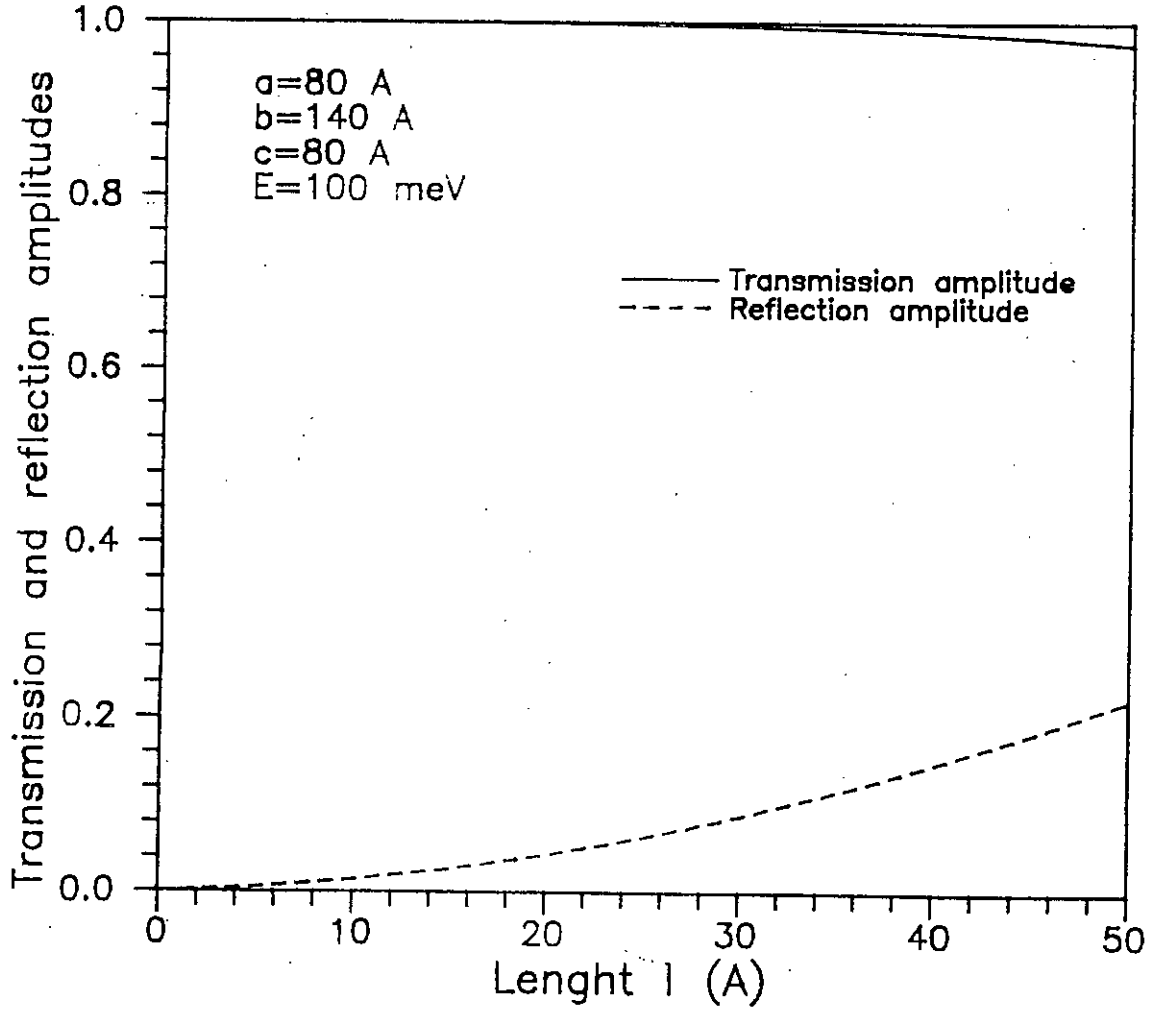

Figure (3.08). Transmission and Reflection amplitudes as a function of channel length in region II for an electron energy of 100 meV.

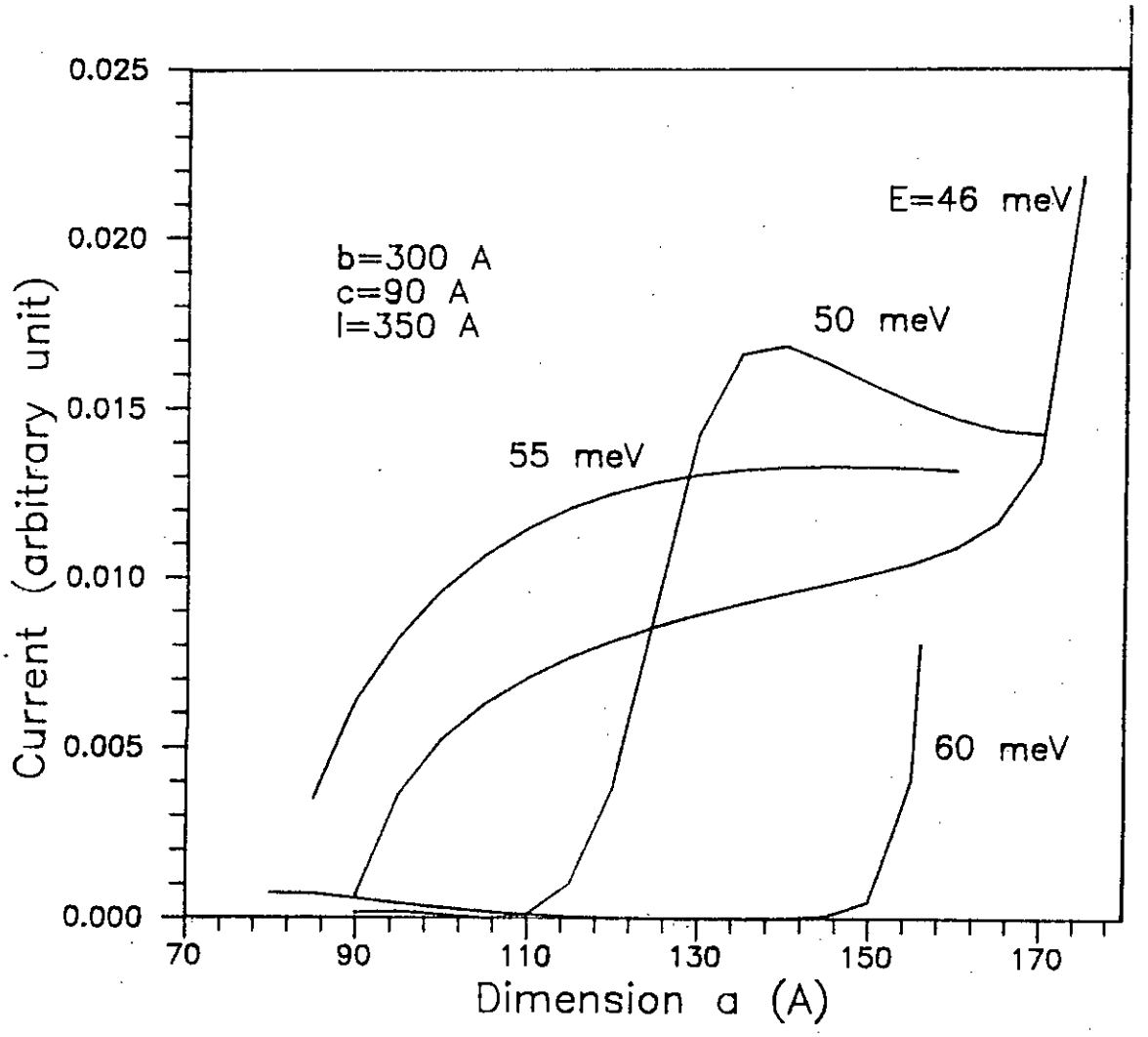

Figure (3.09). Plots of current versus channel width in region I as a function of electron energy. The channel width and length in region II are 300 A and 350 A, respectively.

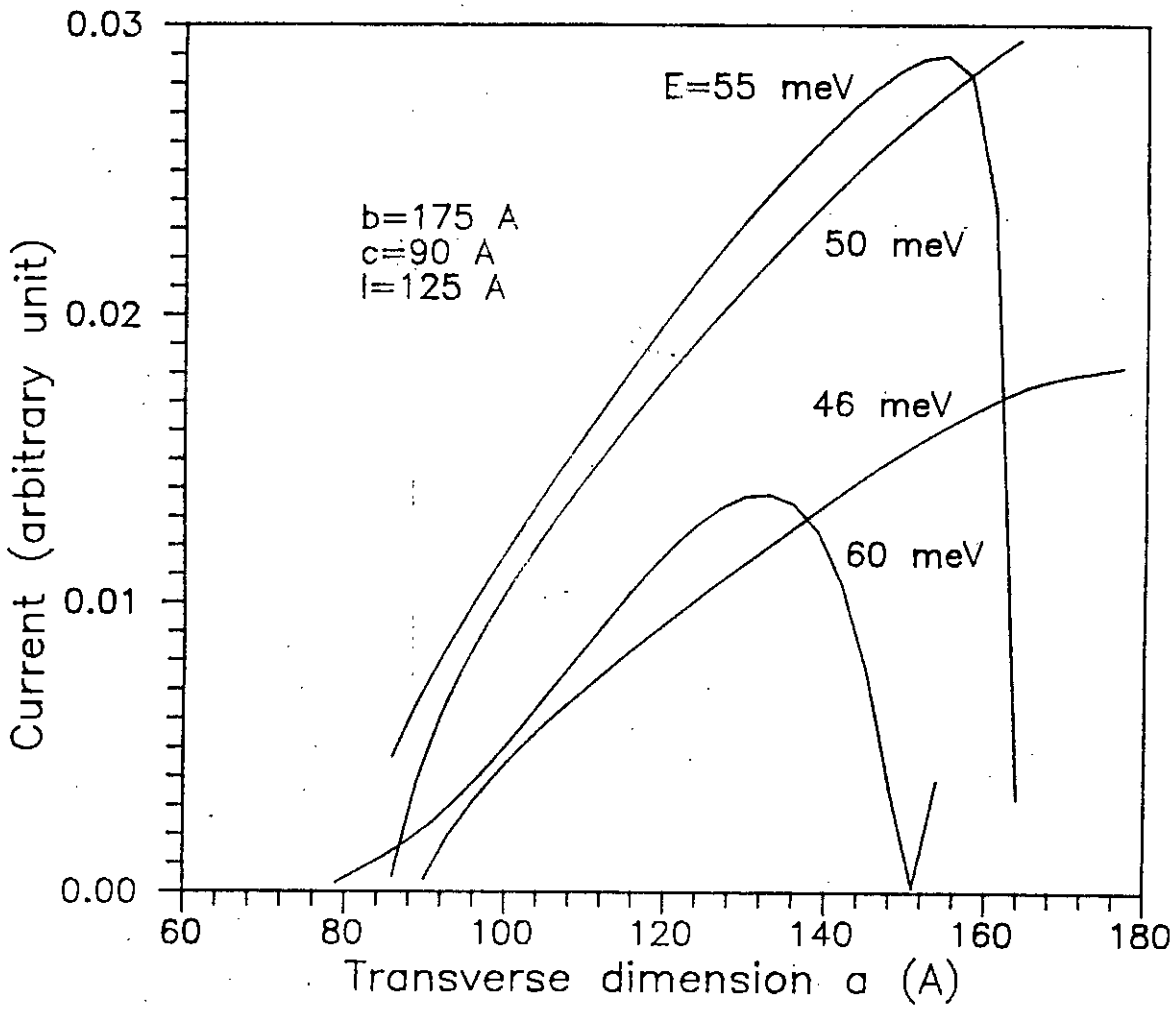

Figure (3.10). Plots of current versus channel width in region I as a function of electron energy. The channel width and length in region II are 175 A and 125 A, respectively.

3.3.3 EFFECT OF VARYING THE WIDTH OF REGION II

We chose the structure shown in fig (3.11), where the width of the intermediate region is varied and effect of this variation on current is calculated and is shown in figure (3.12). With the increase of width 'b' number of modes propagating in region II increase, so we have a strong interference in region II, resulting in a random variation of current.

3.3.4 EFFECT OF VARYING THE WIDTH OF REGION III

We take a structure with a=80 Å, b=140 Å and l=250 Å and the variation of current with transverse dimension c is calculated for four different energies as shown in the figure (3.13). Current is found to vary randomly. However reducing the length l and increasing the width b, a smooth and consistent variation of current can be obtained as shown in the figure (3.14). The structure chosen has a=90 Å, b=175 Å and l=125 Å. A family of curves is shown in fig (3.15) showing variation of current with c for different energies. The chosen structure has a=60 Å, b=100 Å and l=250 Å. In this case number of modes in each of the three regions is 1. Hence there is no interference and variation of current is not much.

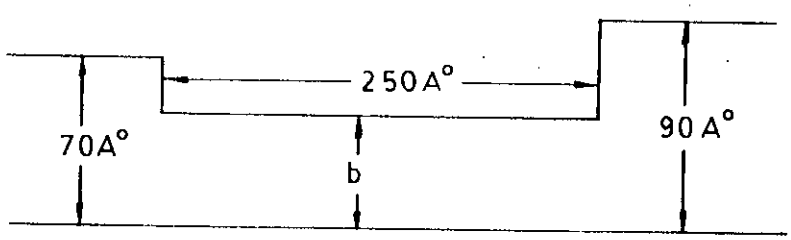

Figure (3.11). Transverse dimensions of a potential channel with double discontinuities in the transverse plane.

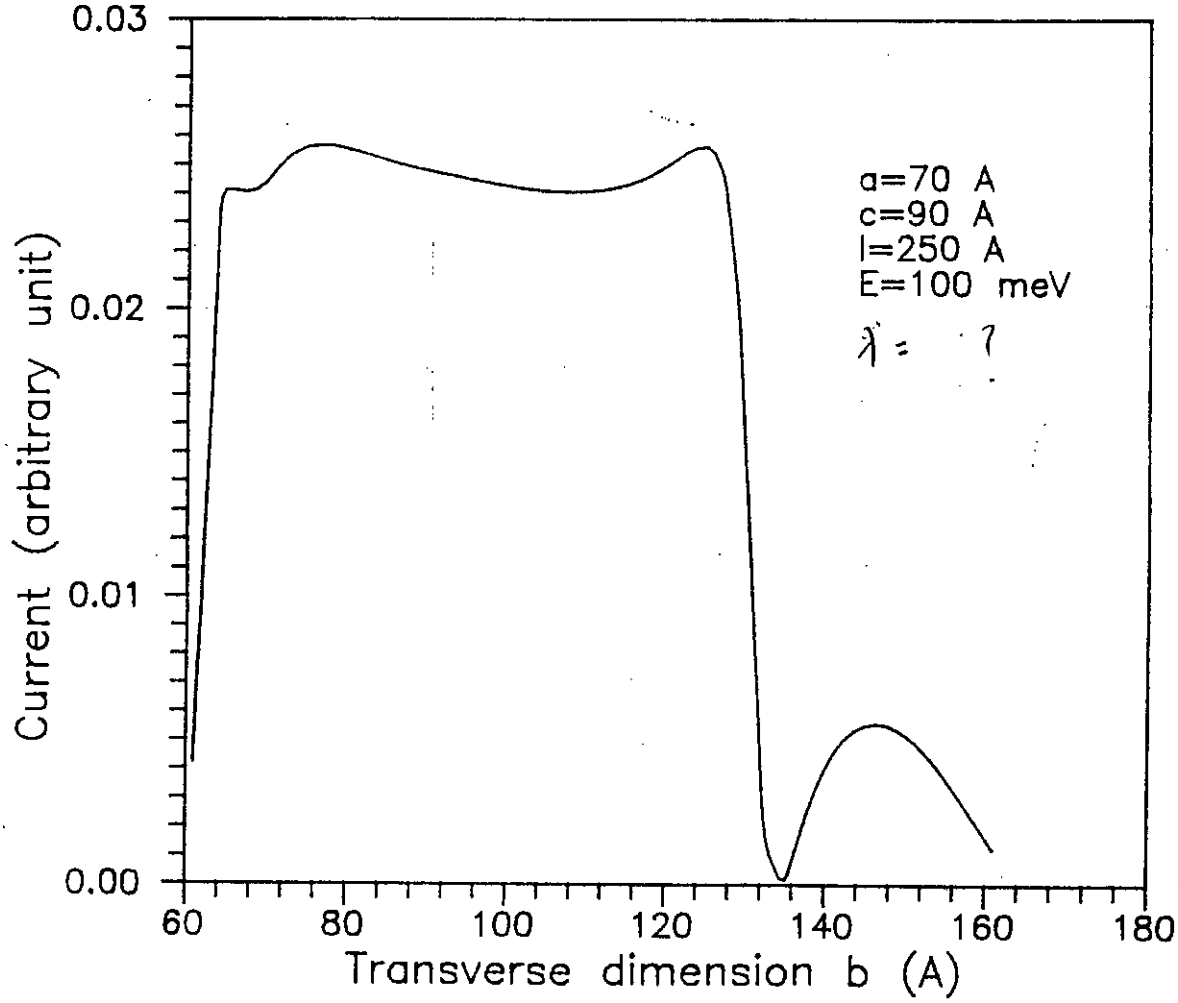

Figure (3.12). A plot of current versus channel width in region II for an electron energy of 100 mev.

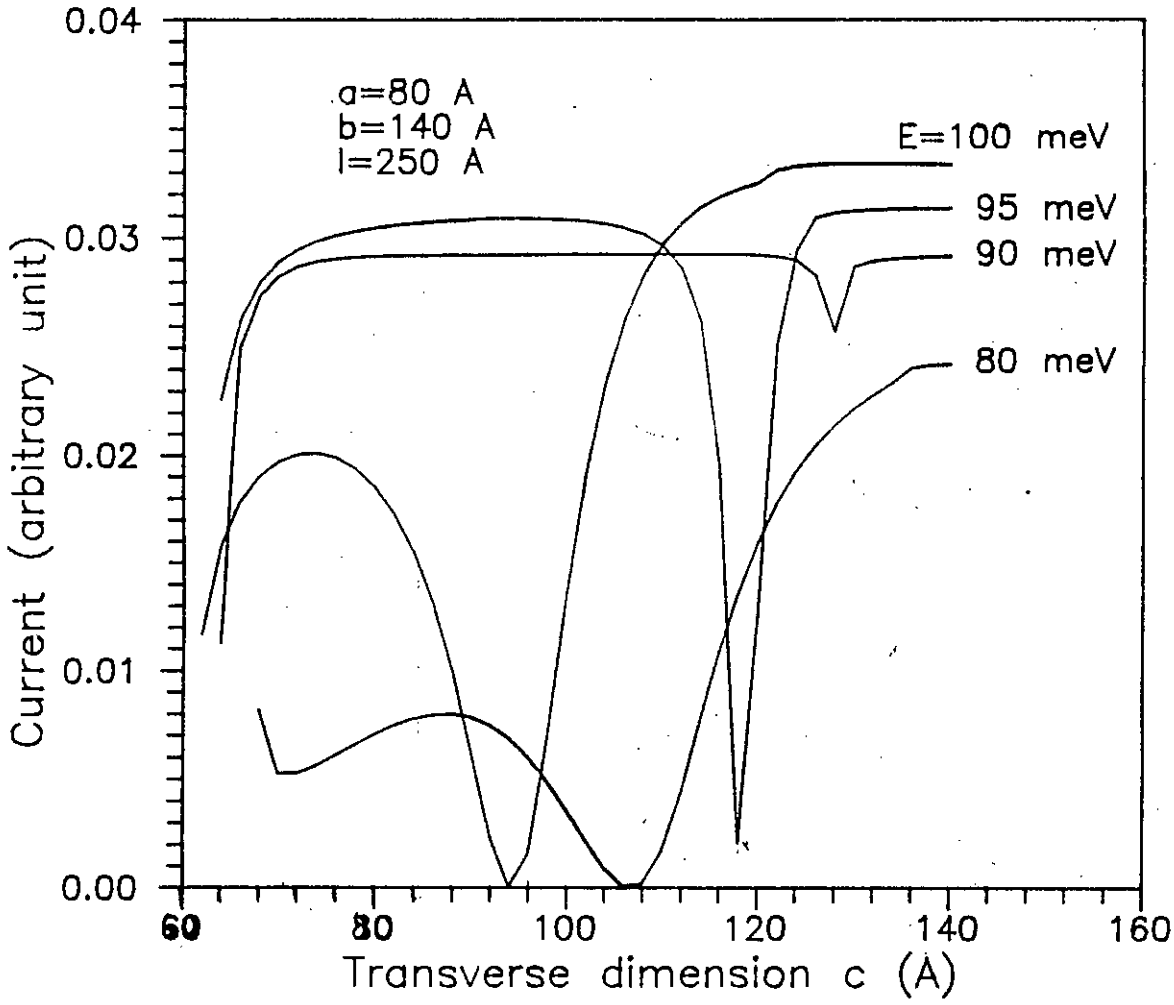

Figure (3.13). Plots of current versus channel width in region III as a function of electron energy.

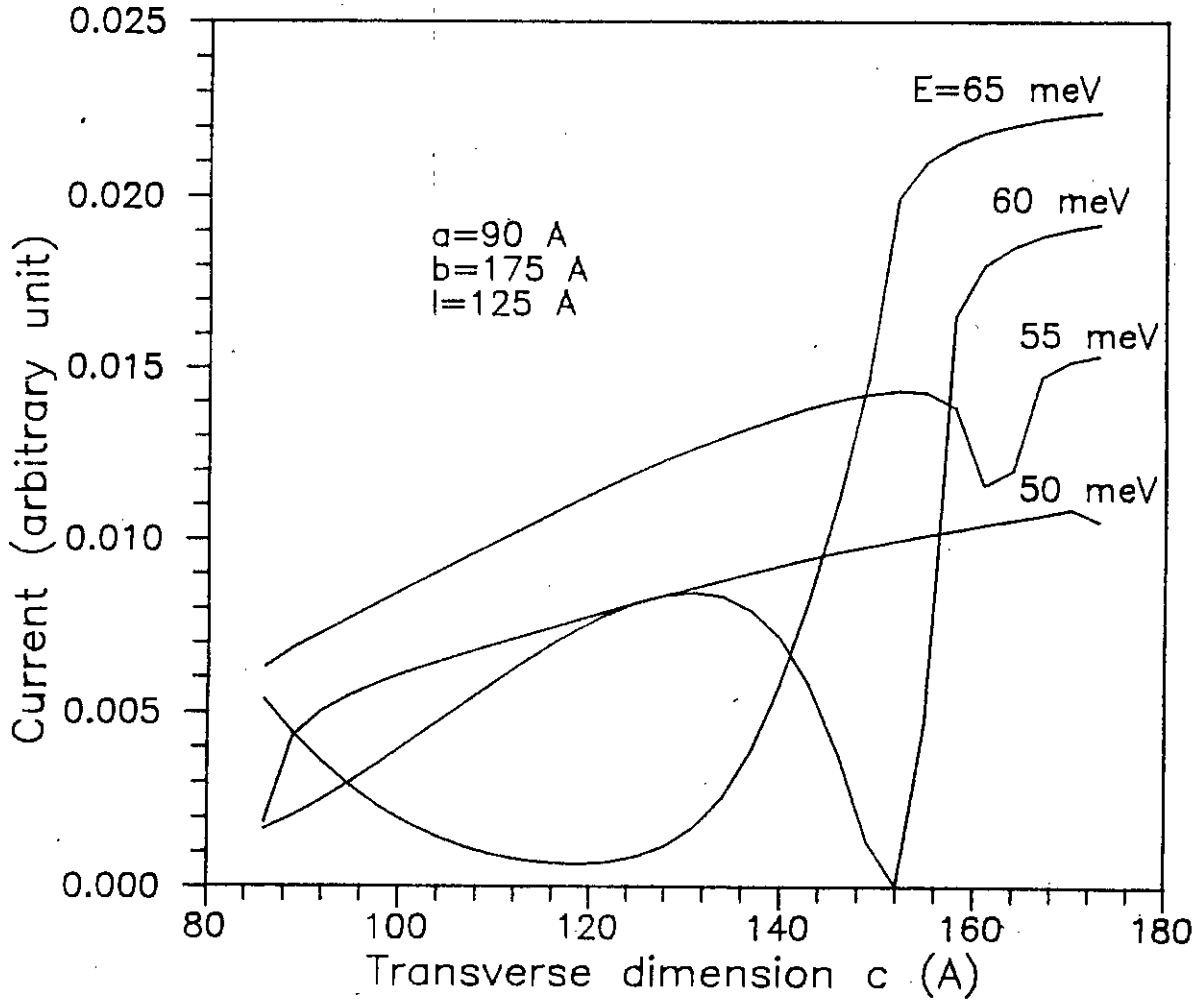

Figure (3.14). Plots of current versus channel width in region III as a function of electron energy.

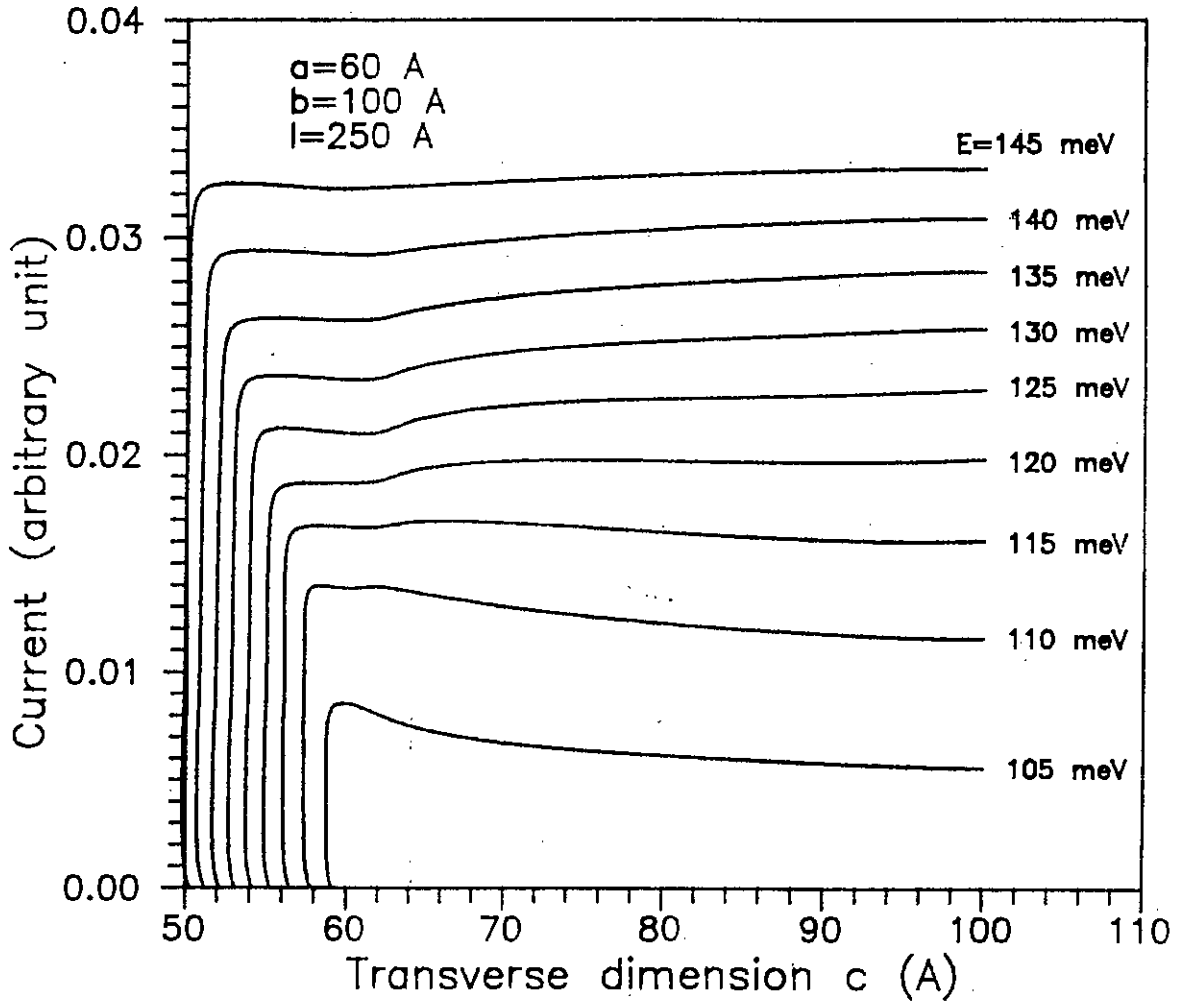

Figure (3.15). Plots of current versus channel width in region III as a function of electron energy.

3.3.5 EFFECT OF CHANNEL POSITION VARIATION OF REGION I AND REGION III

We finally observe the effect of the channel position variation of the 1st and 3rd region, on current. The structures those have been chosen are shown in figure (3.16). Since the two structures are identical the effect of channel position variation on current should also be identical. From fig (3.17) and (3.18) we observe an identical variation of current for both the cases.

3.4 DISCUSSIONS

From the results obtained in this chapter we see current in a structure can be varied widely by varying different dimensions of the structure. The intermediate region in between the two discontinuities plays the most important role in the variation of current. The interference between different modes in this region governs mostly the shape of the curves. Moreover the decaying modes in this region also have a denominating part on the current, they also contribute to the current flow. The discontinuities give rise to cross coupling of the modes which may result in a higher amplitude of the reflected wave compared to the transmitted one. This cross coupling along with the interference of the modes control the magnitude of the current. The most important feature of this current variation is that, by a proper choice of

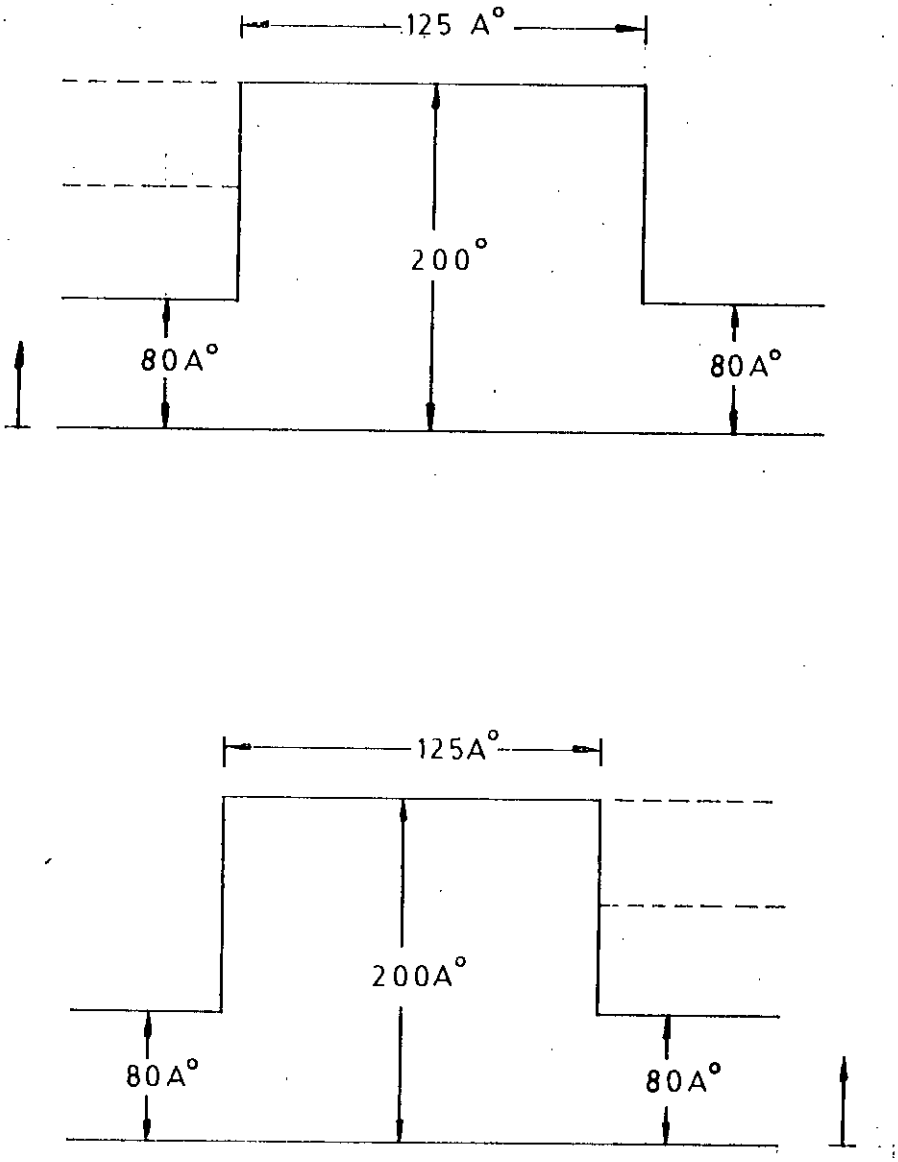

Figure (3.16). Potential channel structures used to study the effect of varying the channel positions in regions I and III on the current.

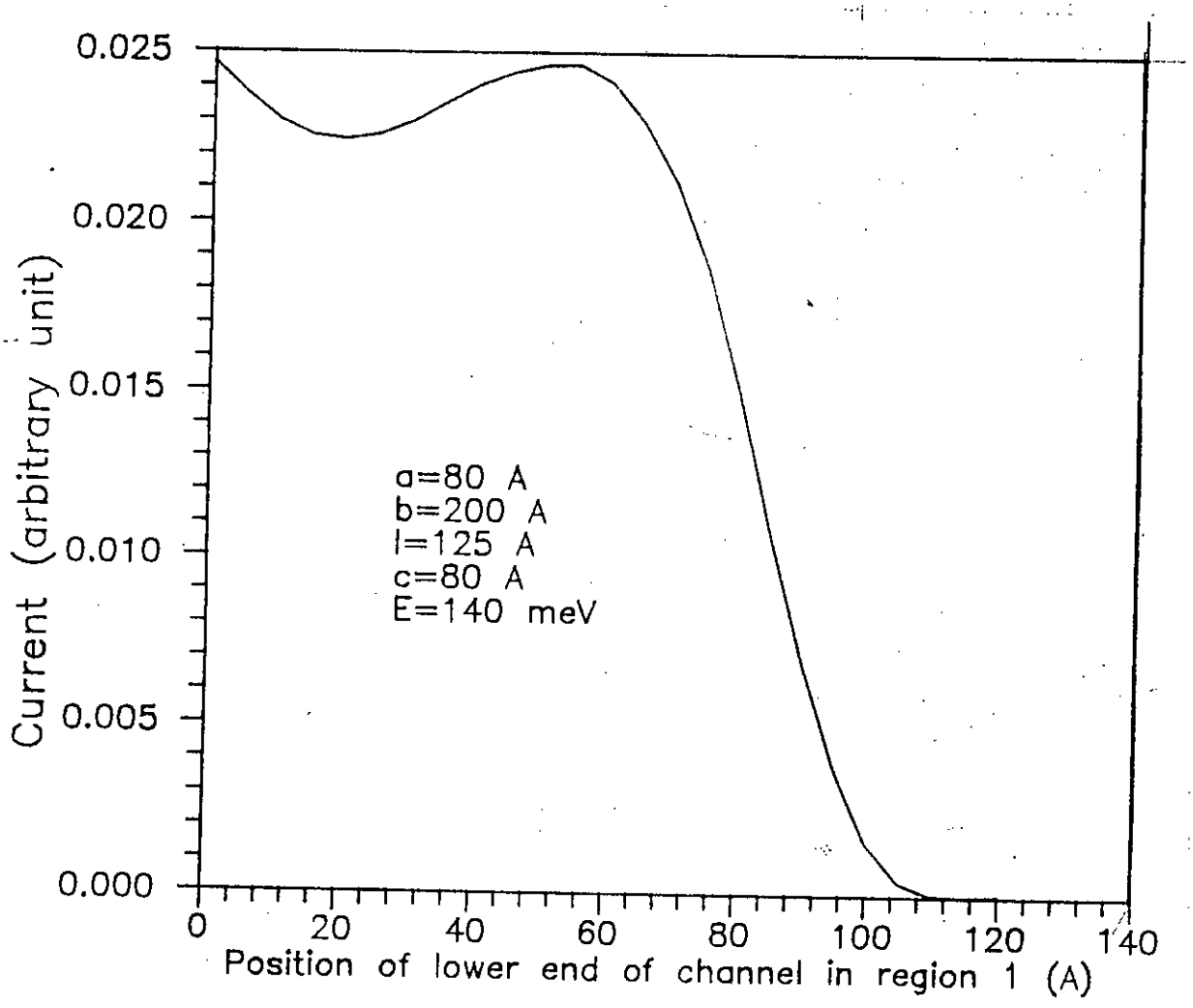

Figure (3.17). A plot of current versus position of the lower end of channel I for an electron energy of 140 meV.

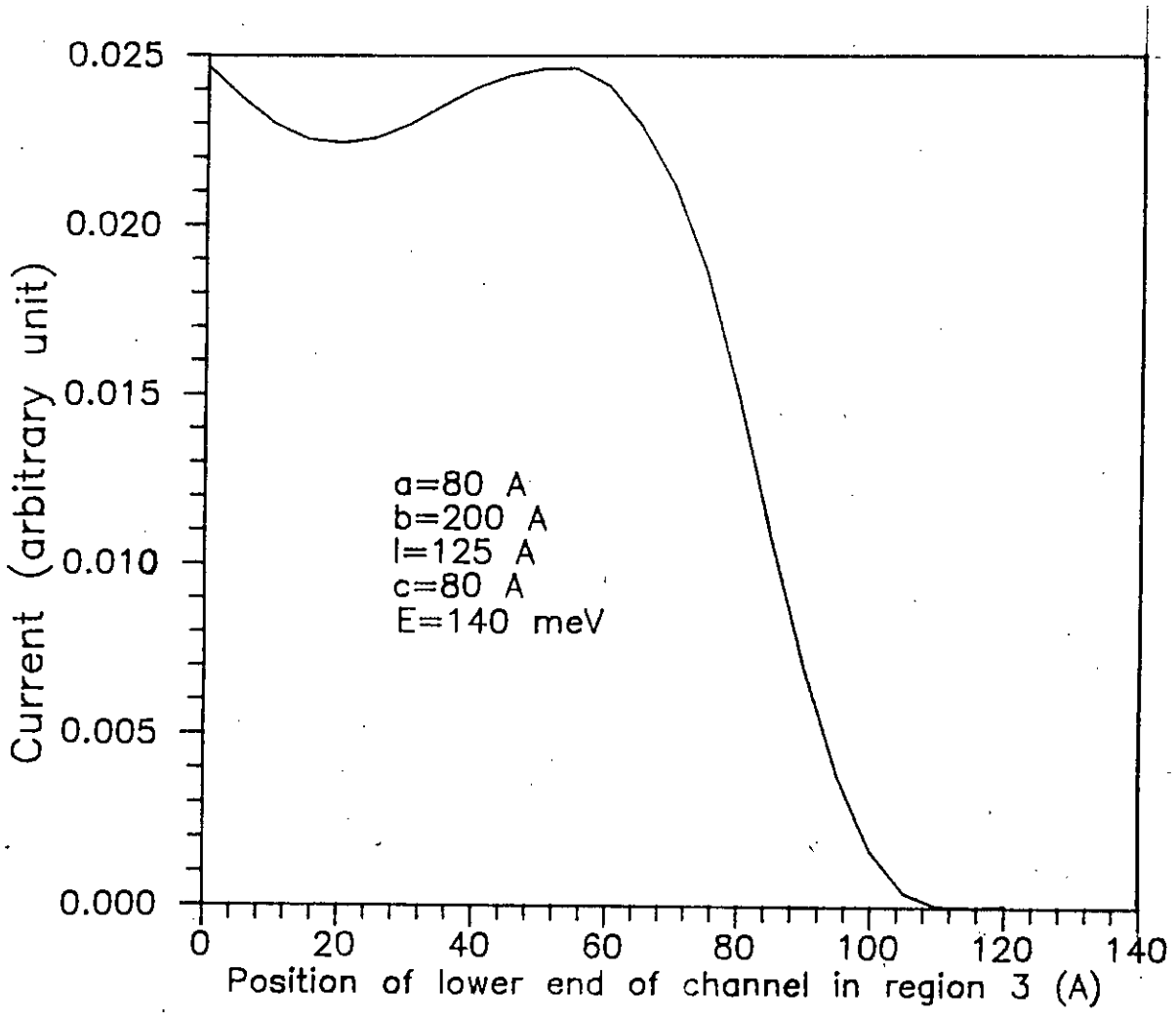

Figure (3.18). A plot of current versus position of the lower end of channel III for an electron energy of 140 meV.

channel dimensions the interference between modes can be controlled and a consistent variation of current for different energies can be obtained which can have interesting practical applications.

CHAPTER FOUR
POSSIBLE DEVICE APPLICATION

4.1 INTRODUCTION

From the results obtained in chapter 3 it has been found that for certain choice of channel parameters, variation of current in the channel is consistent with the variation of dimensions. As mentioned earlier, this variation of current is mainly due to the interference among various modes in region II (fig. 3.02). Choosing channel dimensions properly this interference among the modes can be controlled. The channel dimensions can be varied by applying voltage externally. If the rate of change of current with respect to the applied voltage is large then the device can be used as an amplifier. The possibility of using the device as an amplifier is studied in this chapter.

4.2 A PROPOSED AMPLIFIER

The basic structure of the proposed amplifier is shown in figure 4.01(a). Two gates are placed on the structure separated by a distance l. With the application of negative voltage (considering n type channel) at the gates, channels near the gates will be constricted due to the charge depletion. An abrupt depletion layer is assumed (fig. 4.01 b) and the change in potential profile is considered to be rectangular (fig. 4.01 c). Hence three distinct segments of channels are obtained having different widths. In figure 4.01 (b) a and c are the width of the channels at region I and region III respectively b and l are the width and length of channel at region II.

We have seen in chapter 3, the interference of different modes in region II determines the shape of the current variation. In order to avoid an erratic

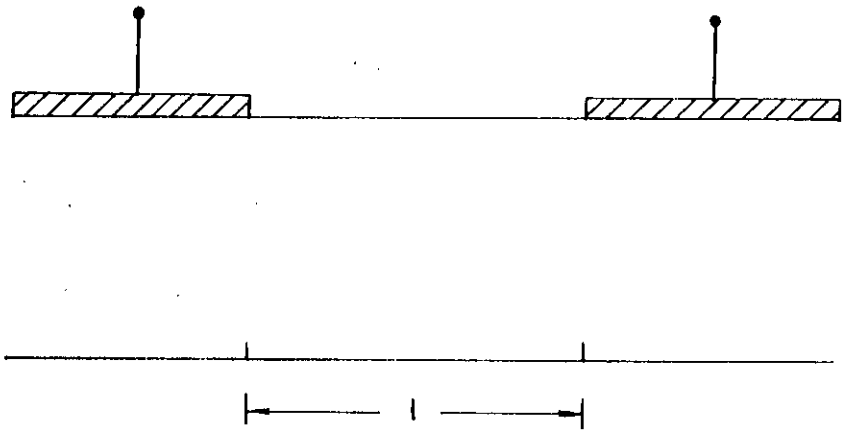

Figure (4.01a). The basic structure of the proposed amplifier.

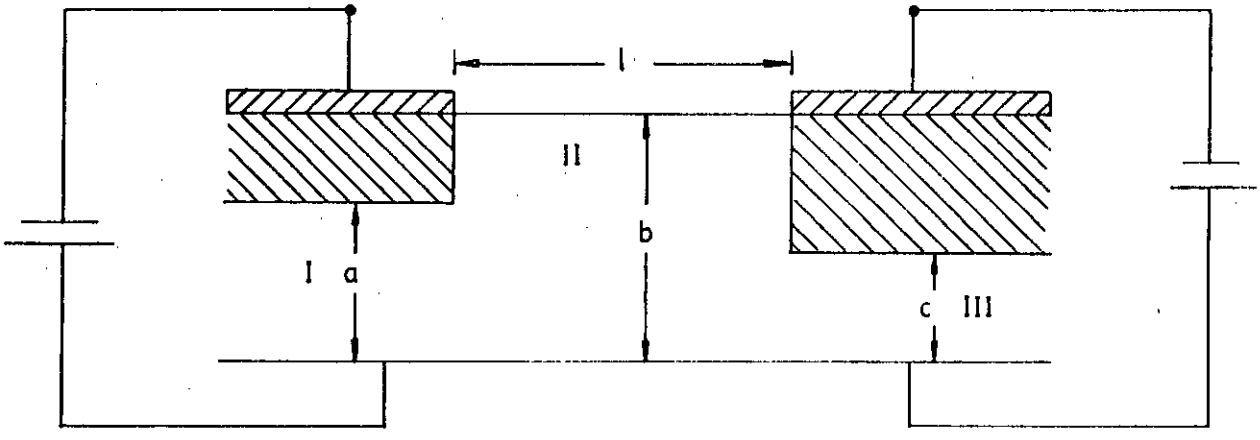

Figure (4.01b). A schematic diagram illustrating the effect of gate voltages on the potential profile of figure (4.01a).

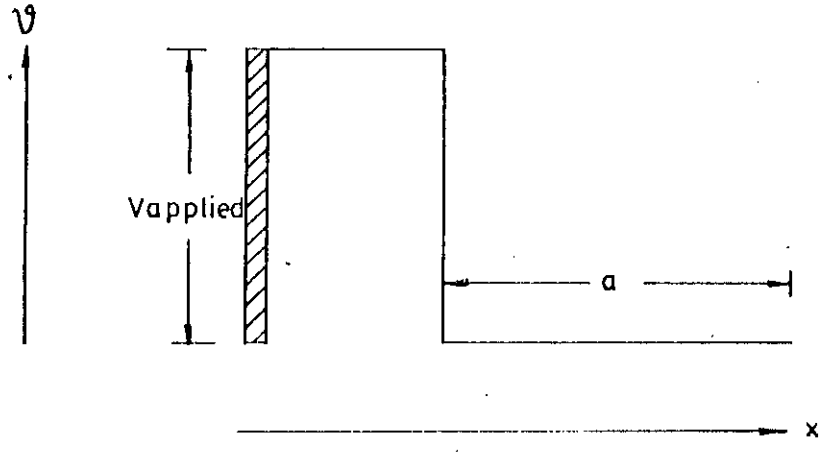

Figure (4.01c). The assumed potential profile.

variation of current resulting from interference among various modes, number of propagating modes in region II is reduced to some controllable number. This can be done by reducing the width of this region thereby lowering the probability of higher mode propagation. Length of the channel of this region is also chosen to be small in order to control the phase of the interfering modes.

Choice of the width of region I is also important. Reducing the channel width adequately, probabilities of higher mode propagation can be lowered considerably. Only the fundamental mode is considered to be propagating in region I. Higher propagating modes are avoided since the phase constants of the incoming higher modes are unknown. However reduction of the channel width of region I will also reduce the current flow, hence width of this region must be chosen carefully.

Abrupt depletion layer which is assumed earlier, is not practically achievable. In practice formation of depletion layer is more gradual as has been shown in figure 4.02 (a). The assumption of rectangular potential profile is also an approximation. The actual potential profile will change gradually with x, as shown in figure 4.02 (b). However a sharp depletion can be achieved by increasing the doping density inside the channel. The analysis that follows are based completely on the assumption of abrupt depletion and rectangular potential profile.

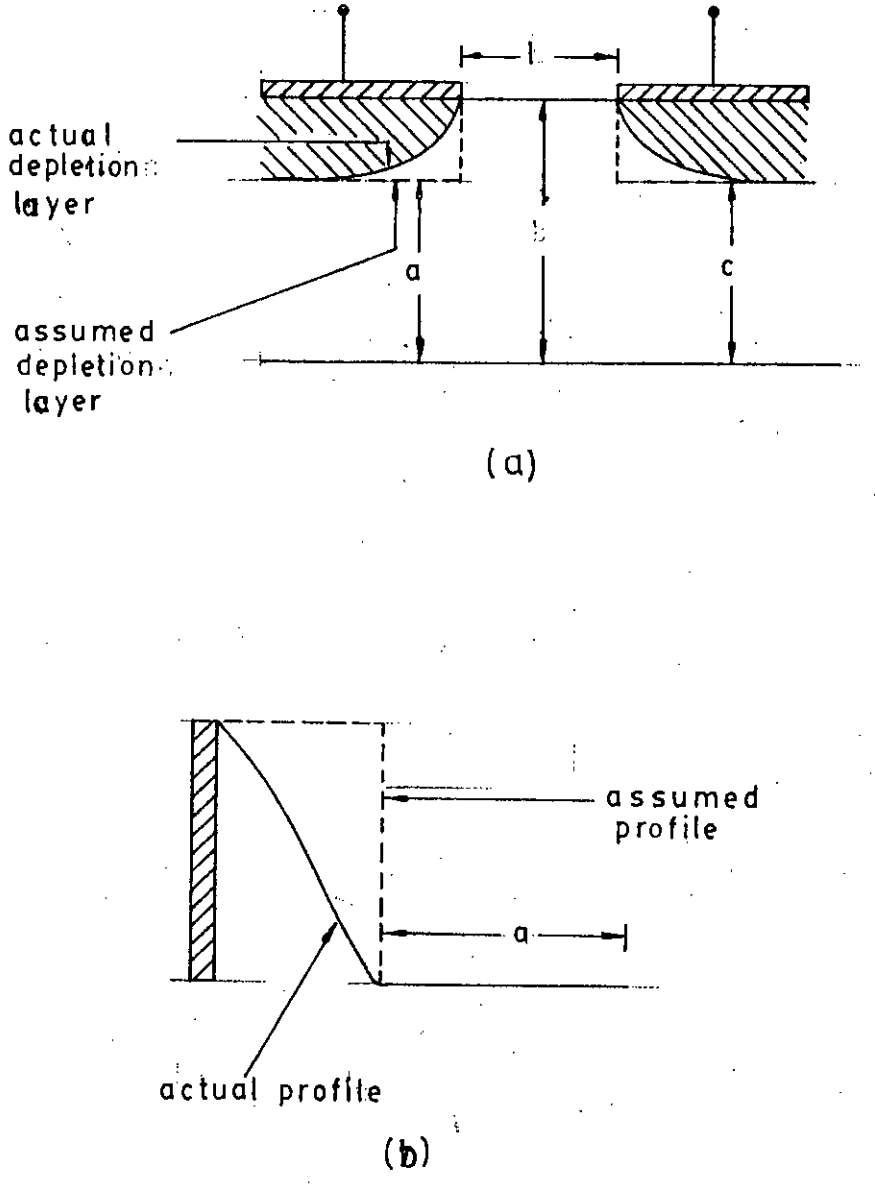

Figure (4.02). Actual and approximated potential variation in the depletion layer.

4.3 MATHEMATICAL FORMULATION FOR CURRENT

Wave function Ψ in the channel can be written as

$$\Psi = \Psi_x(x)\Psi_z(z) \tag{4.01}$$

where wave function Ψ has a spatial distribution in x (bound in this direction by potential barrier), is propagating in the z direction and is invariant in y.

The probability current s in the channel is given by the relation [11]

$$s = \Re\left(\Psi^* \frac{h}{2im'} \nabla\Psi\right) \tag{4.02}$$

where

$$\nabla = \hat{i}\frac{\partial}{\partial x} + \hat{j}\frac{\partial}{\partial y} + \hat{k}\frac{\partial}{\partial z}$$

and $\Re$ stands for real part.

Since Ψ is invariant in y and is bound in the x direction, current per meter of the y direction is given by

$$\Re\int_{-\infty}^{\infty}\left(\Psi_x^{*}\Psi_x\right)dx\,\frac{eh}{2im^{*}}\frac{\partial\Psi_z(z)}{\partial z}\Psi_z^{*}(z)$$

(4.03)

since Ψ_x is normalized the integral

$$\int_{-\infty}^{\infty}\left(\Psi_x^{*}\Psi_x\right)dx=1$$

(4.04)

Using the relation (3.01) current in the channel for a particular mode n can be determined as

$$I=\frac{eh}{2m^{*}}k_{1n}\left(1-\lambda_{nn}{}^{2}\right)$$

(4.05)

where k_{1n} is the wave vector in z direction and λ_{nn} is the reflection amplitude.

This current is contributed by a single electron having a wave vector k_{1n}

Actual current contribution of the electron having wave vector k_{1n} can be calculated by multiplying equation (4.06) by the number of electrons available.

Actual number of available electrons can be determined from the knowledge of

the density of state and the Fermi Dirac probability of occupancy.

The two dimensional density of states changes by $m'/\pi\hbar^2$ [12] (fig. 4.03) at each energy E_{1n} for which a new subband appears. For the fundamental mode density of state g(E) is given by

$$g(E) = \frac{m'}{\pi\hbar^2} \quad (4.06)$$

where E is the sum of the kinetic energies due to the motion of electrons in y and z direction. It is interesting to note that two dimensional density of state is independent of energy.

According to Fermi Dirac distribution the probability of occupancy with total energy E_t is given by

$$f(E_t) = \frac{1}{1 + e^{(E_t - E_F)/kT}} \quad (4.07)$$

where E_F represents the fermi energy, k is the Boltzmann's constant T is the absolute temperature and E_t is the total energy of electron given by

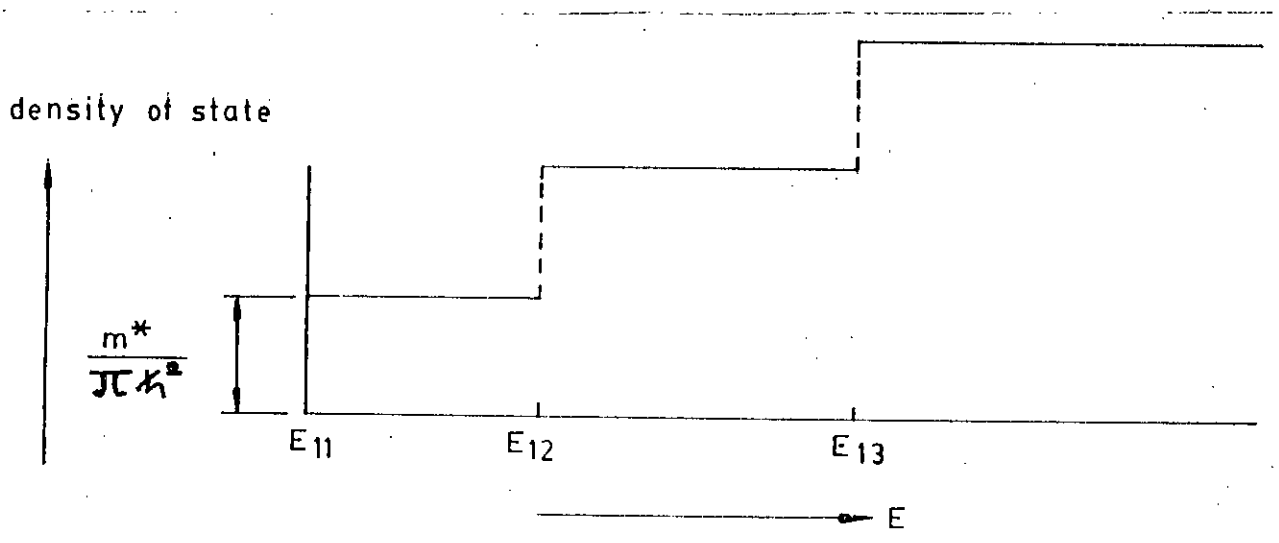

Figure (4.03). The two-dimensional density of state function.

$$E_t = E + E_z$$

(4.08)

here E_z is the eigen energy.

Total number of electrons available over an energy element dE is given by

$$n(E)dE = f(E_t)g(E)dE$$

(4.09)

For a given value of k_{1n}, k_y can vary from 0 to ∞. Hence the absolute propagating constant k can be expressed as $k = \sqrt{k_{1n}^2 + k_y^2}$, which makes an angle θ with k_{1n} as shown in figure (4.04). From the figure, we can also express k as

$$k = \frac{k_{1n}}{\cos\theta}$$

(4.10)

Hence, the total energy, corresponding to the propagation constant k is

$$E_t = \frac{\hbar^2 k^2}{2m^*} + E_{1n}$$

$$= \frac{(k_{1n}/\cos\theta)^2 \hbar^2}{2m^*} + E_{1n}$$

(4.11)

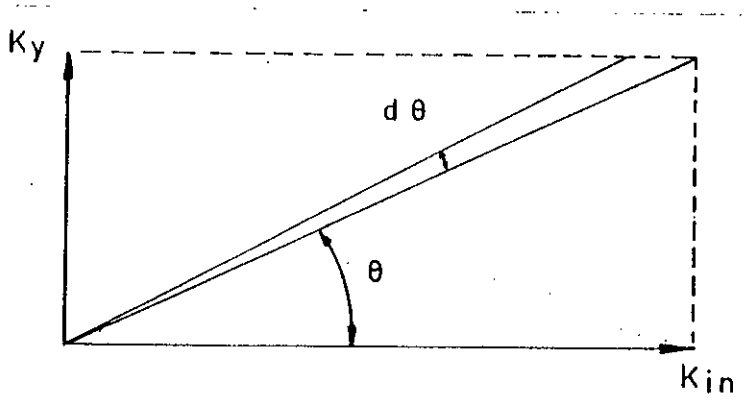

Figure (4.04). A diagram illustrating the relationship between wave vectors in different directions.

Using relation (2.06) we have

$$E_t = E_z / \cos^2\theta + E_{1n}$$

(4.12)

where E_z is the energy of electron due to the motion of electron in the z direction.

The total number of electron having a propagation constant k_{1n} in the z direction and making an angle θ in the k diagram (4.04) can be expressed as

$$N(E)\,d\theta\,dE_z = g(E_z)\,f(E_t)\,d\theta\,dE_z$$

(4.13)

Hence, number of electrons having propagation constant k_{1n} is

$$N(E_z)\,dE_z = \left[\int_{-\pi/2}^{\pi/2} \{g(E_z)\,f(E_t)\}\,d\theta\right] dE_z$$

(4.14)

current contributed by these electrons is obtained by multiplying equations (4.14) and (4.05)

$$dI = \frac{eh}{2m^*} g(E_z) k_{1n}\left(1 - \lambda_{nn}^{\ 2}\right) \int_{-\pi/2}^{\pi/2} \frac{d\theta\, dE_z}{1 + e^{(E_t - E_F)/kT}} \tag{4.15}$$

Total current in the channel is now given by

$$I = \frac{eh}{2m^*} \int_0^{\infty} \left[g(E_z) k_{1n}\left(1 - \lambda_{nn}^{\ 2}\right) \int_{-\pi/2}^{\pi/2} \left\{ \frac{1}{1 + e^{(E_t - E_F)/kT}} \right\} d\theta \right] dE_z \tag{4.16}$$

TIME RESPONSE

The ultimate speed of operation of the device will depend on the time required for the wavefunction to reach its steady state value. The total charge enclosed in the device divided by the rate at which charge is flowing will give the build-up time [13]

$$\tau_d = \frac{\int_0^{\infty} \left[\int_0^{l} \left\{ \int_{-\infty}^{\infty} \left(e\Psi^{\ 2} N(E) \right) dx \right\} dz \right] dE}{I} \tag{4.17}$$

4.4 RESULTS

The structure we choose first has the dimensions b=200 Å, l=100 Å and c=120 Å. The signal is applied at the gate at region I. In our calculation we have assumed a doping density of $2X10^{17}cm^{-3}$, an effective mass of $0.067m_o$ and a T of 300° K. The location of the fermi level with respect to the conduction band edge can be determined by the relation [14]

$$E_F = -kT\ln\left(\frac{N_c}{N_d}\right) \tag{4.19}$$

taking the bottom of the conduction band to be zero. Where N_c is the effective density of states in the conduction band and N_d is the doping density.

The calculated values of the channel current as a function of channel dimension is shown in figure (4.05). The dimension axis of the curve can be converted to a voltage axis by using the relation [15]

$$V = \frac{qN_d}{2\epsilon_r\epsilon_0}x^2 \tag{4.20}$$

which relates the width of the depletion layer x to the gate voltage V. Here ϵ_r is the relative permittivity of the material of the channel.

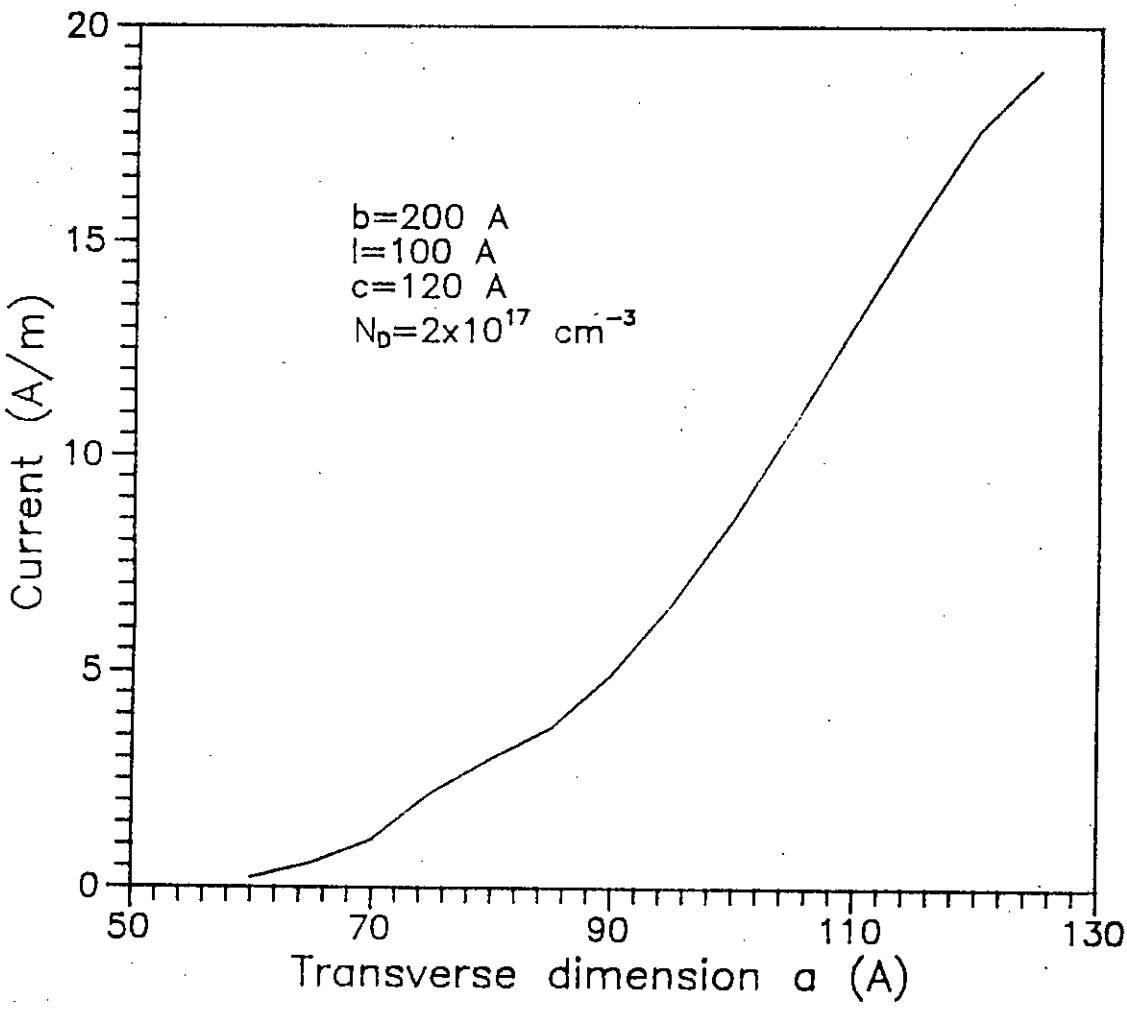

Figure (4.05). Calculated current as a function of channel width in region I for a doping density of $2x10^{17}$ cm^{-3}.

While calculating the gate voltage contact potential between the gate and the channel is neglected. Rescaling the dimension axis of the figure (4.05) in terms of the applied voltage, the variation of current with the gate voltage is found as shown in the figure (4.06). The linear portion of the curve in figure (4.06) can be used to amplify a signal without appreciable distortion. Transconductance g_m calculated from this linear portion of the curve is found to be 1600 ampere/volt per meter length in the y direction. Considering a length of 1 micron in the y direction g_m is found to be 1.6 ma/volt which is reasonably a high value and is comparable to the transconductance of the field effect transistors. A time response of .0885 pico second is obtained for the chosen parameters. This fast time response will enable a high speed operation of the device.

Changing the doping density of the current structure to $4.7X10^{17}cm^{-3}$ a variation of current with the channel dimension is calculated and is shown in figure (4.07). The corresponding variation of current with the gate voltage is shown in figure (4.08). Transconductance calculated from the linear region of the curve is found to be 1800 mho per meter. Time response is also calculated and a response of .08836 pico second is obtained.

The next structure we choose has the dimensions a=100 Å, b=200 Å and l=125 Å. The signal is applied to the gate at region III. The assumed doping density is $2X10^{17}\ cm^{-3}$. The variation of current with channel dimension c and applied

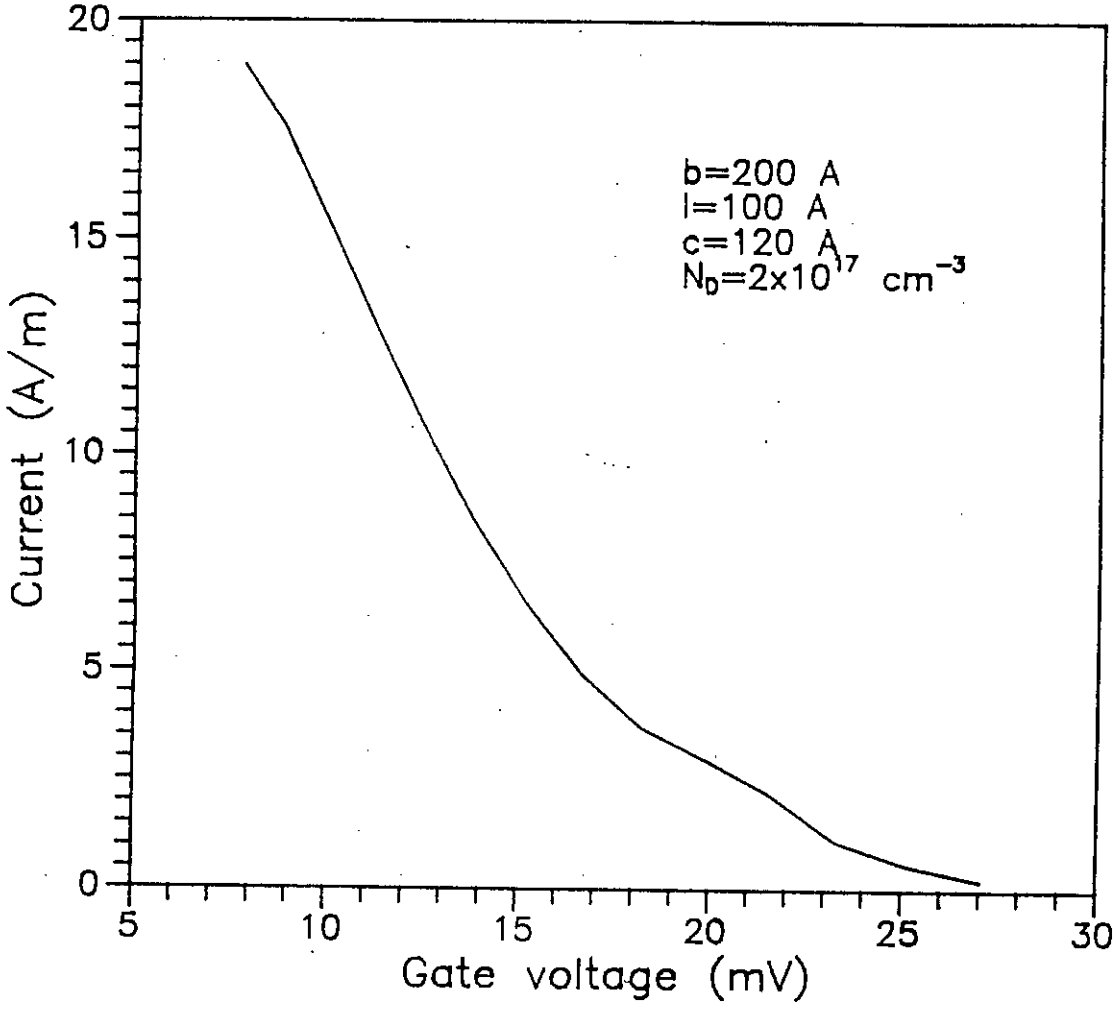

Figure (4.06). Variation of current with voltage applied at the gate of region I for a doping density of $2x10^{17}$ cm^{-3}.

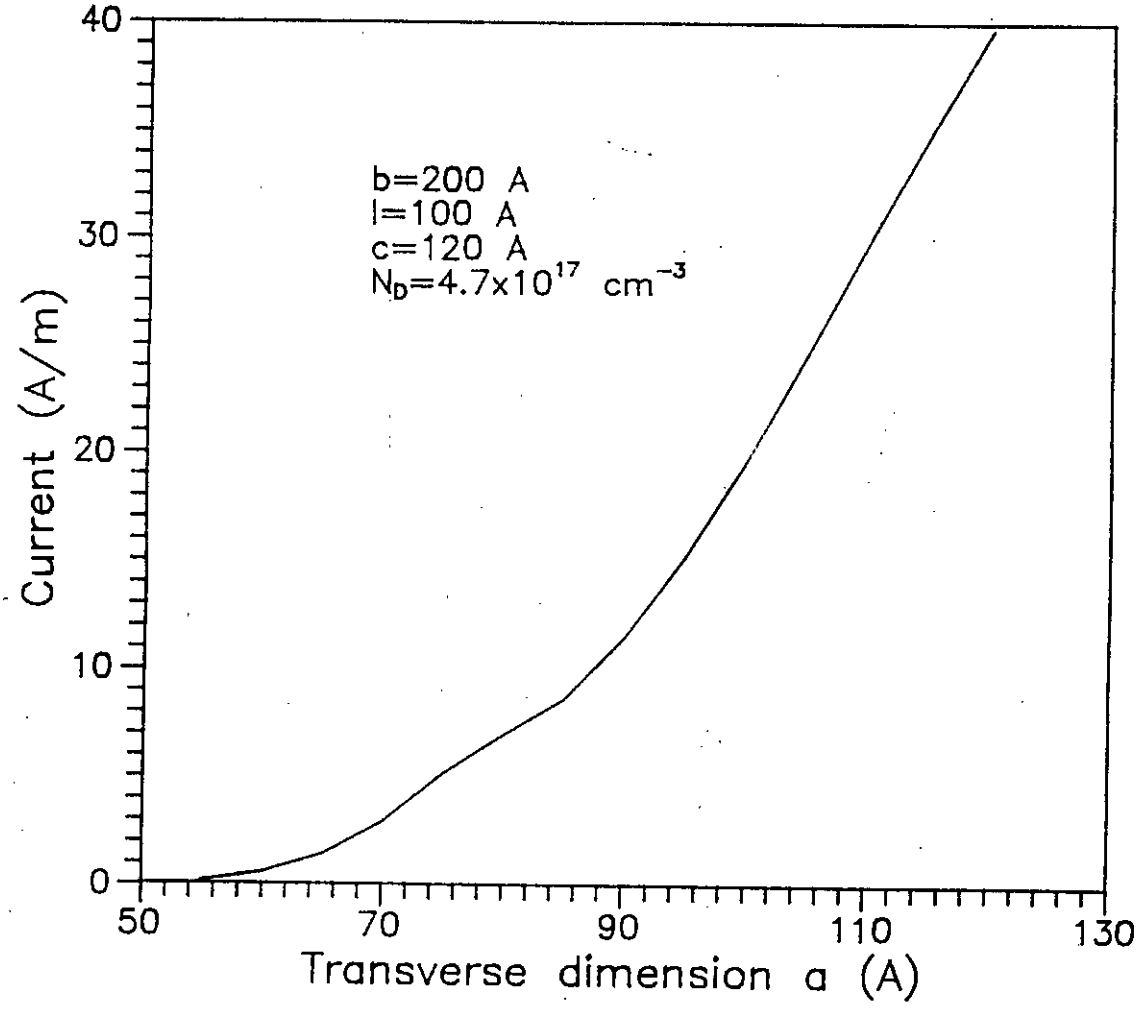

Figure (4.07). Calculated current as a function of channel width in region I for a doping density of 4.7×10^{17} cm^{-3}.

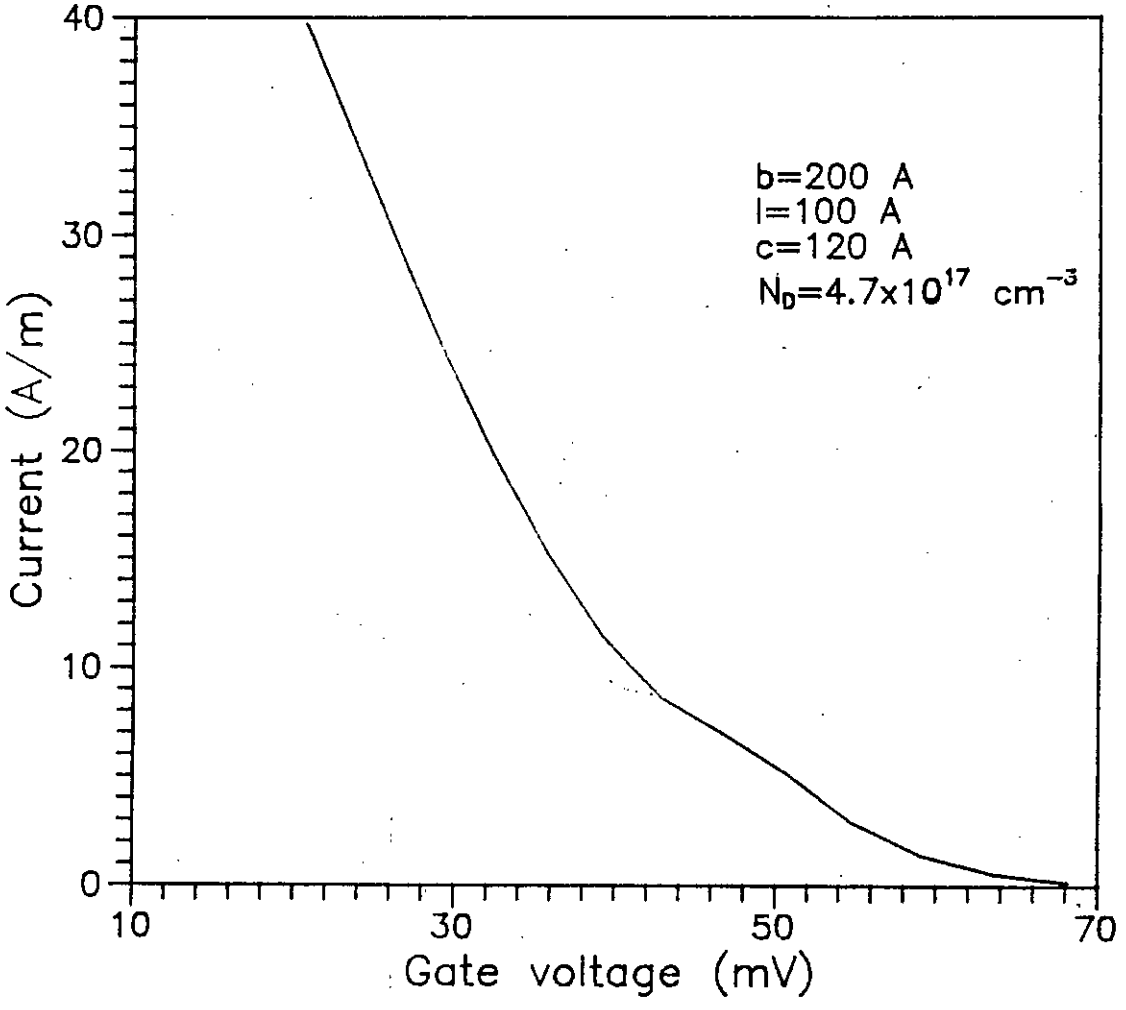

Figure (4.08). Variation of current with voltage applied at the gate of region I for a doping density of 4.7×10^{17} cm^{-3}.

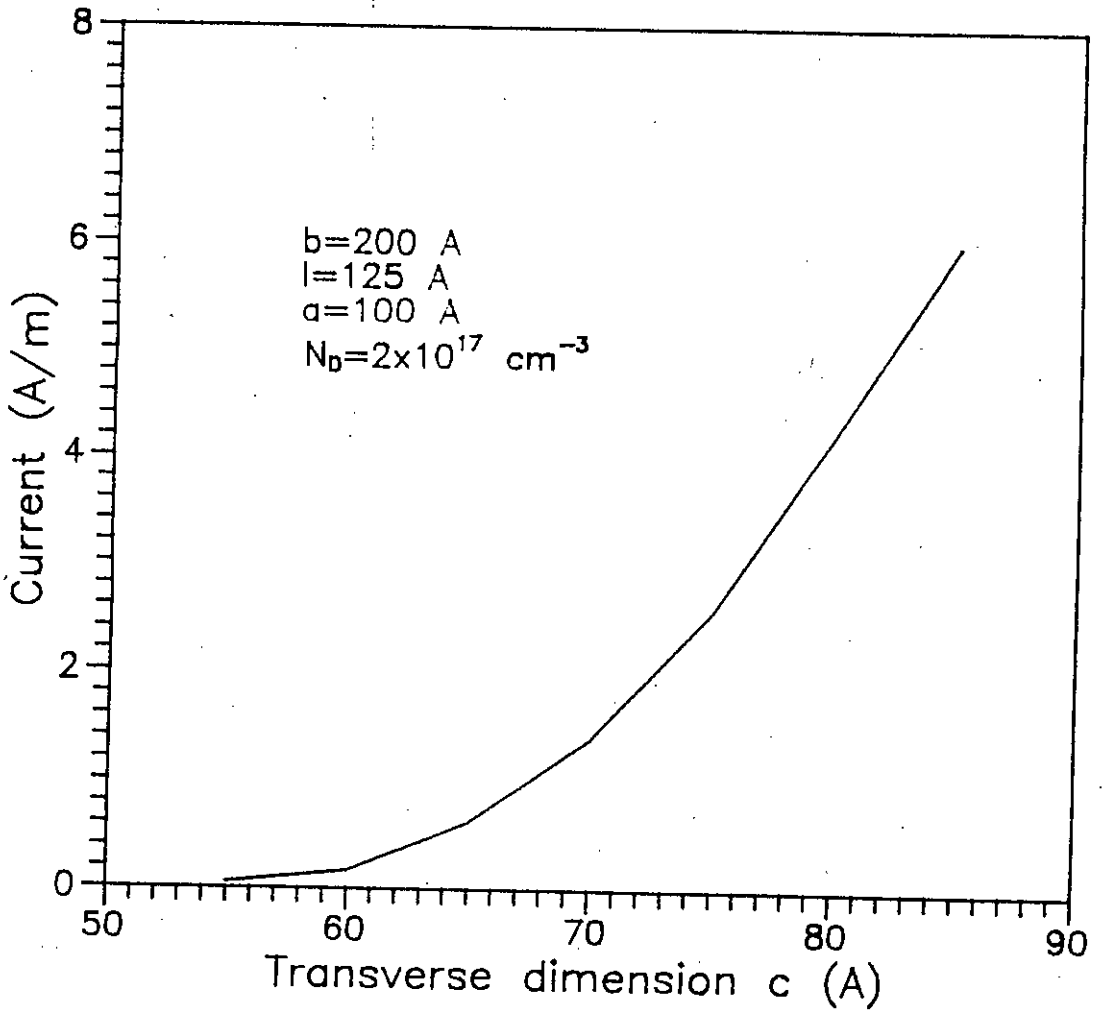

Figure (4.09). Calculated current as a function of channel width in region III for a doping density of $2x10^{17}$ cm^{-3}.

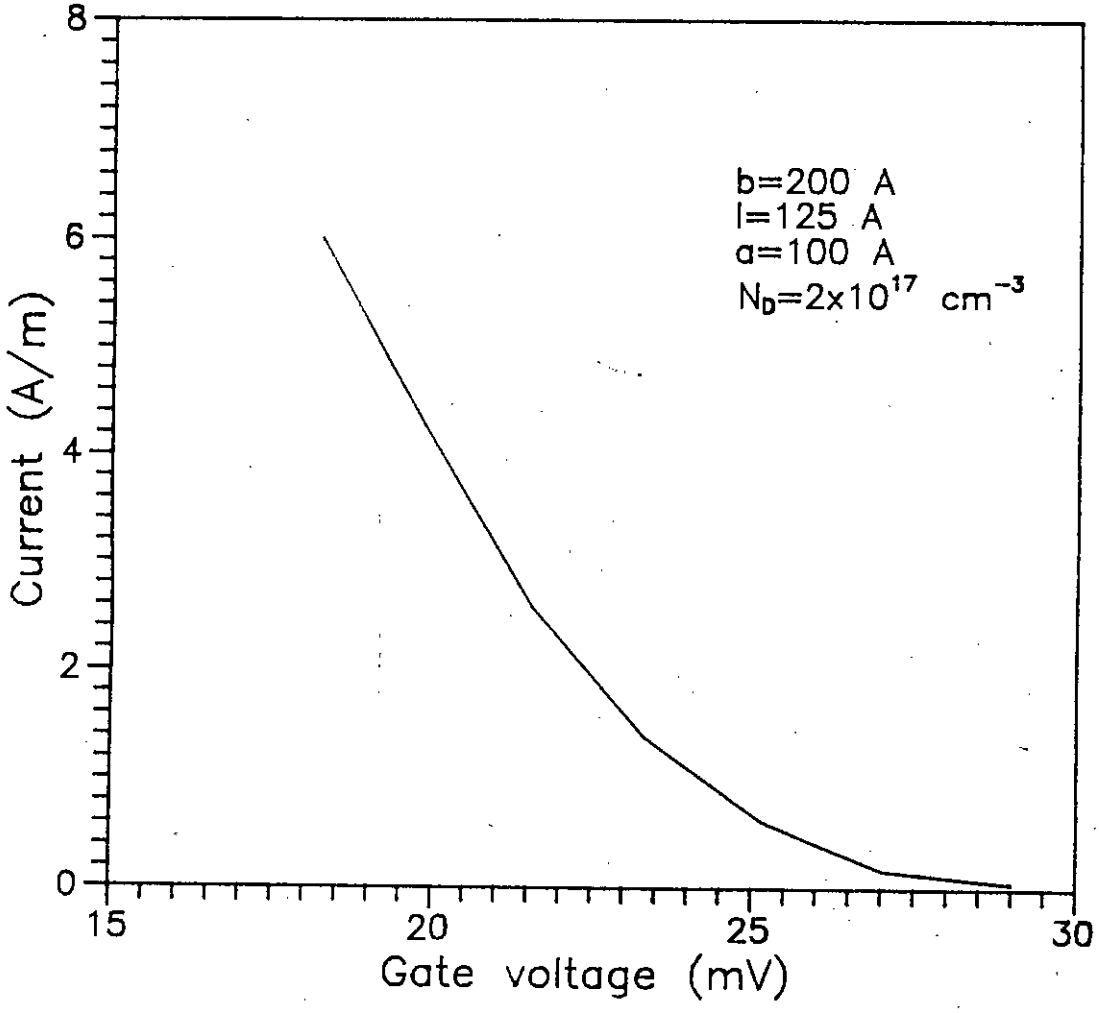

Figure (4.10). Variation of current with voltage applied at the gate of region III for a doping density of $2x10^{17}$ cm^{-3}.

voltage V is shown in the figures (4.09) and (4.10) respectively. Transconductance calculated from the curve of figure (4.10) is found to be 1076 mho per meter.

DISCUSSION

When channel dimensions and other parameters (doping density, channel material etc.) are chosen carefully, the device is found to exhibit high transconductance and faster time response which will make the device applicable in high gain and high frequency operations.

CHAPTER FIVE

CONCLUSION

5.1 SUMMARY

Theoretical analysis have been performed to study the electron propagation process in ultrathin potential microstructures, discontinuous in a plane transverse to the propagation direction. Mathematical model has been formulated to solve single as well as double discontinuous channel problems. The method is developed based on the microwave theories on waveguide discontinuity. The developed method solves the wave function at the discontinuities and in the channel regions quite accurately.

An illustrative result is presented in chapter 2 showing the dependency of the reflection and transmission amplitude of a single discontinuous channel, on the variation of the channel dimensions. Unity transmission is obtained while the discontinuity is removed. This shows the validity of the method developed.

Numerous results on double discontinuous channels are presented in chapter 3. The variation of the channel current on the channel dimensions are thoroughly investigated. A sharp variation of current with change in channel dimensions is observed. The interference among various modes controls mainly the shape of the current variations. By controlling the interference a consistent variation of current is obtained.

An attempt is made to use the double discontinuous channel as an amplifier using simplifying assumptions. Some results are presented in chapter 4 illustrating the performance of the device as an amplifier. The transconductance was found to be reasonably uniform over a considerable

range of current. Transit time of the order of 10^{-13} sec is obtained. This fast response along with the high gain might make the device applicable in various high speed, high gain operations.

5.2 SUGGESTION FOR FUTURE WORK

The results presented in this work are based completely on the assumptions of rectangular potential structure with infinite potential barrier in the transverse direction. However the methods formulated are generalized and can be applied to potential structures of arbitrary shapes containing finite barrier. But in this case the overlapping constants $\{A_{mn}, B_{mn}\}$ are to be evaluated numerically by solving the Scrödinger equations at the boundaries.

The mathematical models are developed assuming an abrupt transition between different regions. But in real devices transitions are more gradual. Such a gradual junction can be approximated as a succession of abrupt junctions. A set of equations for each junctions can be obtained, then by solving all the equations as a whole, overall performance of the graded junction can be obtained. But this procedure will increase the computational time considerably.

The method presented here calculates the eigenfunctions of potential structure at the absence of any external electrical field. On the application of the external electric field the entire potential profile will be tilted. However the problem of electron transport in the potential structure can be solved taking the tilting of the potential structure into account.

REFERENCES

1. T. Ando, A. B. Fowler, and F. Stern, "Comprehensive review on electronic properties of Two-Dimensional systems," Rev. Mod. Phys. 54, p.437, 1982.

2. Proceding of the fifth international conference on electronic properties of two-dimensional systems (Oxford,1983).

3. S. Datta, S. Bandyopadhyay, M. R. Mellah, R. Reifenberger, M. Miller and M. Vaziri, "Aharonov-Bohm oscillation due to quantum interference between parallel quantum wells," Surf. Sci. 174, pp.439-443, 1986.

4. S. M. F. Kabir, "Quantum mechanical analysis of potential channel structures for current divider amplifier," M. Sc. thesis submitted to the department of EEE, BUET, Octobar 1988.

5. A. M. Kriman and P. P. Ruden, "Electron transfer between regions of quasi two-dimensional and three-dimensional dynamics in semiconductor microstructures," Phys. Rev. B 32, pp.8013-8020, 1985.

6. R. Frohne and S. Datta, "Electron transfer between regions with different confining potentials," J. Appl. Phys. 64, pp.4086-4090, 1988.

7. L. Lewin, "On the resolution of a class of waveguide discontinuity problem by the use of singular integral equations," IRE Tran. Microwave theory and Tech., pp.327-332, 1961.

8. L. I. Schiff, Quantum mechanics (McGraw-Hill, 1968), ch.6.

9. L. I. Schiff, Quantum mechanics (McGraw-Hill, 1968), ch.3.

10. R. Frohne and S. Datta, "Electron transfer between regions with different confining potentials," J. Appl. Phys. 64, pp.4086-4090, 1988.

11. L. I. Schiff, Quantum mechanics (Mcgraw-Hill, 1986), ch.2.

12. D. Delgebeaudeauf and N. T. Linh, "Metal-(n) AlGaAs-GaAs two-dimensional electron gas," IEEE Trans. Electron Devices 29, pp.955-960, 1982.

13. M. Buttiker and Landauer, "Traversal time for tunneling," Phys. Rev. Lett. 49, pp.1739-1742, 1982.

14. S. M. Sze, Physics of Semiconductor Devices (Wiley Eastern, 1980), ch.1.

15. P. A. H. Hart, Handbook of Semiconductors, Ed. C. Hilsum, ch.2.

APPENDIX A

DERIVATION OF THE EXPRESSION FOR CURRENT IN REGION II

Current in the channel per unit length in y direction is given by the relation (4.02)

$$I = \Re \int_{-\infty}^{\infty} \left(\psi^{*} \cdot \frac{e\hbar}{im^{*}} \frac{\partial \psi}{\partial z} \right) dx \qquad (A.1)$$

Wave function for region II is given by the relation (3.02). Assuming number of propagating modes in region II to be l and replacing jk_{2n} by γ_{2n} for the nonpropagating modes we have

$$\frac{\partial \Psi(x,z)}{\partial z} = -j \sum_{n=1}^{l} k_{2n} T_{2n} \Psi_{2n}(x) e^{-jk_{2n}z} + j \sum_{n=1}^{l} k_{2n} R_{2n} \Psi_{2n}(x) e^{-jk_{2n}(l-z)}$$

$$- \sum_{m=l+1}^{\infty} \gamma_{2n} T_{2n} \Psi_{2n}(x) e^{-\gamma_{2n}z} + \sum_{m=l+1}^{\infty} \gamma_{2n} R_{2n} \Psi_{2n}(x) e^{-\gamma_{2m}(l-z)} \qquad (A.3)$$

The limit of integration of equation (A.1) for region II is from 0 to b, since outside the channel electron eigenfunction vanishes everywhere.

Using equation (3.02) and (A.3) in equation (A.1) and integrating we have

$$I = \frac{eh}{m^*} \sum_{n=1}^{l} k_{2n} \left\{ T_{2n}{}^2 - R_{2n}{}^2 \right\}$$

$$+ \Im \sum_{m=l+1}^{\infty} \left[\gamma_{2m} e^{-\gamma_{2m} l} \left\{ T_{2m} R_{2m}^* - R_{2m} T_{2m}^* \right\} \right] \qquad (A.4)$$

where the symbol $\Im$ means the imaginary value

APPENDIX B

DERIVATION OF THE EXPRESSION FOR CONSTANTS A_{mn}, B_{mn}

We determine the expression for the constants $A_{mn} B_{mn}$ considering any arbritrary rectangular potential structure, shown in figure (B.1).

Normalized wave function $\Psi(x)$ for region III can written, using relation (2.25), as

$$\Psi_{3m}(x) = \sqrt{\frac{2}{d-c}} \operatorname{Sin} \frac{m\pi(x-c)}{(d-c)} \qquad (B.1)$$

Similarly wave function for region II is given by

$$\Psi_{2n}(x) = \sqrt{\frac{2}{b}} \operatorname{Sin} \frac{n\pi x}{b} \qquad (B.2)$$

Using relation (3.13) we have

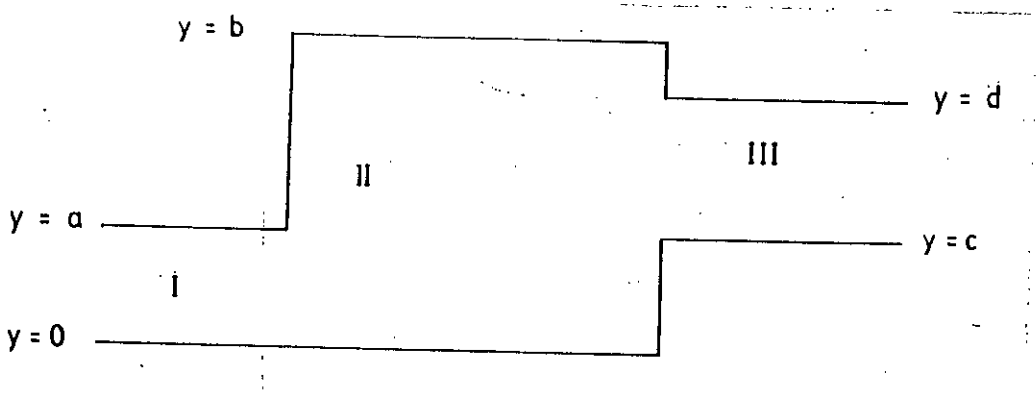

Figure (B.1). The potential structure for the purpose of calculating the overlapping constants.

$$B_{mn} = \int_c^d \frac{2}{\sqrt{b(d-c)}} \mathrm{Sin}\frac{m\pi(x-c)}{(d-c)} \mathrm{Sin}\frac{m\pi x}{b} dx \qquad (B.3)$$

Integrating we get

$$B_{mn} = K\left[(-1)^{m+1}\mathrm{Sin}\frac{n\pi d}{b} + \mathrm{Sin}\frac{n\pi c}{b}\right] \qquad (B.4)$$

where

$$K = \frac{2\sqrt{b(d-c)}bm}{\pi\left[(bm)^2 - \{n(d-c)\}^2\right]} \qquad (B.5)$$

when bm = n(d-c), the expression takes 0/0 form. Using L' Hospitals theorem expression for B_{mn} is found to be

$$B_{mn} = -\sqrt{\frac{1}{b(d-c)}}\left[(-1)^{m+1} d\cos\frac{m\pi d}{d-c} + c\cos\frac{m\pi c}{d-c}\right] \qquad (B.6)$$

Making proper substitution, the same expressions can be used for the constant A_{mn}.